

Accepted Manuscript

Title: Optical discrimination of fluoride and cyanide ions by coumarin-salicylidene based chromofluorescent probes in organic and aqueous medium

Authors: Subrata Kumar Padhan, Mana Bhanjan Podh, Prabhat K. Sahu, Satya Narayan Sahu



PII: S0925-4005(17)31557-5
DOI: <http://dx.doi.org/10.1016/j.snb.2017.08.133>
Reference: SNB 23000

To appear in: *Sensors and Actuators B*

Received date: 19-4-2017
Revised date: 15-8-2017
Accepted date: 16-8-2017

Please cite this article as: Subrata Kumar Padhan, Mana Bhanjan Podh, Prabhat K.Sahu, Satya Narayan Sahu, Optical discrimination of fluoride and cyanide ions by coumarin-salicylidene based chromofluorescent probes in organic and aqueous medium, *Sensors and Actuators B: Chemical* <http://dx.doi.org/10.1016/j.snb.2017.08.133>

This is a PDF file of an unedited manuscript that has been accepted for publication. As a service to our customers we are providing this early version of the manuscript. The manuscript will undergo copyediting, typesetting, and review of the resulting proof before it is published in its final form. Please note that during the production process errors may be discovered which could affect the content, and all legal disclaimers that apply to the journal pertain.

Optical discrimination of fluoride and cyanide ions by coumarin-salicylidene based chromofluorescent probes in organic and aqueous medium

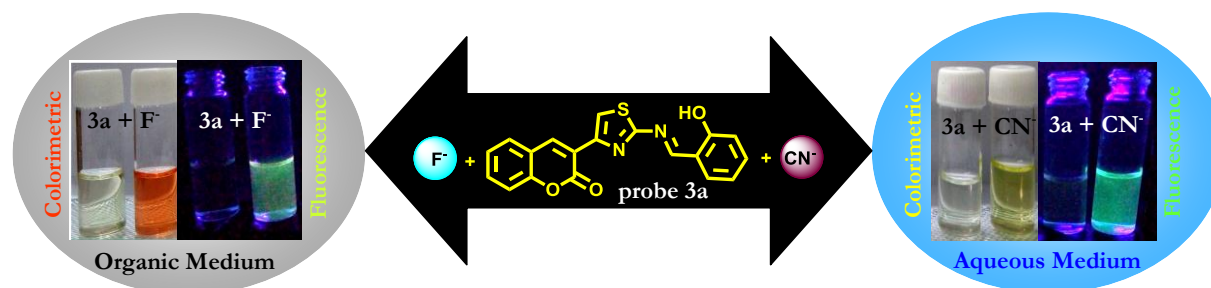
Subrata Kumar Padhan,¹ Mana Bhanjan Podh,¹ Prabhat K. Sahu² and Satya Narayan Sahu^{1*}

¹School of Chemistry, Sambalpur University, Jyoti Vihar, Burla-768 019, Odisha, India

² Center for Multiscale Modelling & Department of Chemistry, National Institute of Science and Technology, Palur Hills, Berhampur-761 008, Odisha, India

Email: snsahu.chem@gmail.com

Graphical Abstract



Highlights

- Chromofluorescent coumarin functionalized salicylidene based probes were synthesized
- Probes detect fluoride ion in organic medium and cyanide ion in aqueous medium
- Detection of fluoride and cyanide ion was achieved both by visible and fluorescence colour change
- Detection limit of fluoride and cyanide ion were at submicromolar and micromolar level
- Cyanide ion can be detected in tap water sample at micromolar level *via* colour and fluorescence change.

Abstract:

Two chromofluorescent coumarin-functionalized salicylidene based probes (**3a** and **3b**) have been synthesized and evaluated for selective detection of fluoride and cyanide ions. Probes **3a** and **3b** selectively detect fluoride ions in acetonitrile medium *via* H-bond interaction and subsequent deprotonation to elicit a distinct visual colour change from colourless to deep red with a significant enhancement in their emission intensity to “turn on” a yellow fluorescence. In addition, probe **3a** could optically discriminate the presence of cyanide ions over other anions by a colour change from colourless to deep yellow with an enhancement of green fluorescence in aqueous-acetonitrile medium (1:1 v/v). Job’s plot experiments revealed a 1:2 binding stoichiometry between the probes and fluoride or cyanide ions. A detailed analysis of the binding characteristics of probe **3a** with fluoride and cyanide ions have been further carried out by ^1H NMR titration studies which indicates a good correlation between colorimetric, UV-visible and ^1H NMR observations. These experimental results were further corroborated from the theoretical models using quantum chemical calculations.

Keywords: Optical sensing, Fluoride ion, Cyanide ion, Chromofluorescent, Organic medium, Aqueous medium

1. Introduction:

Developing specific probes for the solution-based analysis of anionic analytes and mixtures is a challenging task [1-6]. Amongst the various anionic analytes, the detection of biologically and environmentally relevant fluoride and cyanide ions is of most significant [7-9] because the excess use of fluoride can cause dental and skeletal fluorosis while its deficiency can cause osteoporosis in human beings [10, 11]. Similarly cyanide ion plays important roles in many chemical and industrial processes, such as electroplating, plastic manufacturing, gold extraction, tanning, and metallurgy but at the same time it is highly lethal to human health even at a very small concentration due to its strong interaction with the active site of cytochrome-oxidase [12, 13]. Therefore sensing of fluoride and cyanide ions in micro molar concentrations in chemical, biological and

environmental samples is utmost important. Although several methods, including atomic absorption, electrochemical, voltammetric, potentiometric and ion-exchange chromatography techniques have been explored [14-21] but these practices do not offer a cost-effective, rapid and real time-monitoring system for fluoride and cyanide ions.

In this regard the optical chemosensors possessing a chromophoric group are emerged as a powerful tool for the sensing of fluoride and cyanide ions [22, 23]. Majority of these probes are neutral in nature containing acidic hydrogen ($-NH$ or $-OH$) which binds with the fluoride and cyanide ions through hydrogen bonding and subsequently led to colour and/or fluorescence change in the probe solution through a perturbation in their photo physical properties [24-30]. However in the nonpolar aprotic medium there exists an unsolicited interference between fluoride and cyanide ions because of their strong hydrogen bonding ability that ultimately hamper the selectivity in the detection process. This challenge was successfully overcome by using a polar aqueous medium where cyanide ion interacts more preferentially over fluoride ion because of its stronger nucleophilic nature and lower heat of hydration [31]. Therefore modulating the polarity of the sensing medium one can achieve the selective detection of fluoride and cyanide ions in a competitive environment [32, 33]. Moreover sensing of anions in an aqueous environment would pave the way in real time analysis of anions in biological and environmental samples where water is a worth solvent [34, 35]. Based on this concept few reports have been published on selective fluoride and cyanide sensors [36-42], but none of them have reported an optical discrimination in the sensing of fluoride and cyanide ions *via* a dual mode comprise of chromogenic as well as fluorogenic changes.

Recently salicylidine Schiff base derivatives have been emerging as a potential candidate for anion sensors [39, 43-50]. The uniqueness of this molecule is the presence of phenolic OH proton which can act as hydrogen bond donor for anionic species and the azomethine linkage that facilitates to undergo addition type reaction by a nucleophilic anion. Further, the conjugation of the azomethine bond to a chromogenic and/or fluorogenic moiety would provide a photophysical response through efficient charge transfer during anion interaction. It is therefore envisaged that the attachment of a salicylidine unit with a coumarin derivative can lead up to the development of dual mode sensor where the anion interaction may trigger a colour and fluorescence change in the sensor medium. With this vision and in continuation to our efforts towards the development of chromofluorescent

anion sensors [51], we have designed and synthesized two coumarin-thiazolyl functionalized salicylidine probes **3a** and **3b** by simple condensation reactions in high yields. These probes have demonstrated the dual mode detection of fluoride and cyanide ions selectively through an instant visual colour change and fluorescent “turn-on” behavior in organic and aqueous medium respectively. Moreover the binding constants and fluorescence enhancement ratios of probe **3a** and **3b** towards fluoride and cyanide ions were found to be higher than the salicylidine based fluoride and cyanide sensors reported recently [39, 43-45, 48, 50] and exhibit a high level of sensitivity at submicromolar and micromolar concentrations of fluoride and cyanide ions in organic and aqueous medium respectively.

2. Experimental

2.1. Materials

All solvents and reagents (analytical grade and spectroscopic grade) were obtained from Merck (India) and Spectrochem Pvt. Limited (India) and were used without further purification. The required starting materials 3-(2-bromoacetyl)-2*H*-chromen-2-one (**1a**), 2-(2-bromoacetyl)-3*H*-benzo[*f*]chromen-3-one (**1b**) were prepared according to the literature procedures published earlier [52]. The anions such as F⁻, Cl⁻, Br⁻, I⁻, H₂PO₄⁻, HSO₄⁻ and AcO⁻ were used in form of their tetrabutylammonium (TBA) salts whereas CN⁻ was used as KCN salt to study the anion binding properties of probe **3a** and **3b**. All the binding studies carried out in acetonitrile solvent were denoted as organic medium whereas studies carried out in water-acetonitrile (1:1 v/v) mixture solvent were denoted as aqueous medium. 1 mM stock solutions of probe **3a** and **3b** were prepared in UV-grade acetonitrile solvent and were subsequently used for preparation of lower concentrations of the probe solutions through appropriate dilution. The various equivalents of guest anions were added from the stock solutions varying from 10⁻³ to 10⁻⁴ M prepared in organic and aqueous medium. For cyanide ion binding studies in organic medium stock solutions of KCN varying from 10⁻³ to 10⁻⁴ M were prepared in UV-grade DMSO while for studies in aqueous medium, stock solutions of KCN varying from 10⁻³ to 10⁻⁴ M were prepared in Milli-Q water.

2.2. General methods

^1H NMR was recorded on an Avance III-400 MHz Bruker spectrometer. Chemical shifts are reported in parts per million from tetramethylsilane with the solvent (DMSO- d_6 : 2.5 ppm) resonance as the internal standard. Data are reported as follows: chemical shifts, multiplicity (s = singlet, d = doublet, t = triplet, m = multiplet), coupling constant (Hz). ^{13}C NMR (100 MHz) spectra were recorded on an Avance III-400 MHz Bruker spectrometer in proton decoupling mode. Chemical shifts are reported in ppm from tetramethylsilane with the solvent resonance as the internal standard (DMSO- d_6 : 39.51 ppm). UV–visible absorption spectra were recorded on a Shimadzu UV-2450 spectrophotometer. Fluorescence emission spectra were recorded on a Hitachi F-7000 fluorescence spectrophotometer. FT-IR spectra were recorded on a Perkin Elmer RXI spectrometer. pH readings were measured on UTECH CON-700 digital pH meter. Chromatographic purification was done using 60–120 mesh silica gels (Merck). For reaction monitoring, manually coated silica gel-60 TLC plates were used.

2.3. Synthesis of the probe

2.3.1. General procedure for synthesis of precursor **2a-2b**

Solid thiourea (0.456 gm, 2 mmol) was added gradually over three times to a hot (60 °C) solution of 3-bromoacetyl coumarin derivative **1a** (0.534 gm, 2 mmol) or **1b** (0.634 gm, 2 mmol) in ethanol (25 mL) under stirring condition. Initially the solution looked turbid and the solution became clear after complete addition of thiourea. On cooling the reaction mixture to room temperature after 30 min. some crystals were deposited from the reaction mixture which was filtered, washed with cold ethanol and then boiled with water containing 0.3 gm of sodium acetate for 10 mins. The boiling mixture was then allowed to cool to room temperature and the solid product obtained was filtered and then washed with cold water for several times to remove the excess sodium acetate and thiourea if present. Then the products **2a** and **2b** were recrystallized from ethanol and glacial acetic acid respectively to get the desired compounds as needle like crystals in good yields after drying in vacuum (**2a** = 85 %, light green colour and **2b** = 86 %, light yellow colour).

3-(2-aminothiazol-4-yl)-2H-chromen-2-one (2a)

M.P. = 224 °C. ^1H NMR (400 MHz, DMSO- d_6) δ (ppm) = 7.15 (2H, s, NH₂, D₂O exchangeable), 7.34 (1H, t, J = 5.6 Hz, Ar-H), 7.40 (1H, d, J = 6.4 Hz, Ar-H), 7.50 (1H, s, thiazolyl-H), 7.57

(1H, t, $J = 6.0$ Hz, Ar-H), 7.79 (1H, d, $J = 6.4$ Hz, Ar-H), 8.49 (1H, s, coumarinyl-H). ^{13}C NMR (100 MHz, $\text{DMSO-}d_6$) δ (ppm) = 108.7, 115.8, 119.3, 120.4, 124.7, 128.6, 131.4, 138.1, 143.3, 152.1, 158.8, 167.4. ^{13}C -dept-135 ($\text{DMSO-}d_6$) δ (ppm) = 109.2, 116.2, 125.1, 129.1, 131.9, 138.5. FT-IR (KBr) ν (cm^{-1}) = 3381, 3153, 1697, 1643, 1604, 1537, 1450, 1379, 1323, 1267, 1178, 1101, 1006, 923. UV-visible (acetonitrile, 50 μM) = λ_{max} (nm) 372 ($n-\pi^*$).

2-(2-aminothiazol-4-yl)-3H-benzof[*f*]chromen-3-one (2b)

M.P. = 256 $^{\circ}\text{C}$. ^1H NMR (400 MHz, $\text{DMSO-}d_6$) δ (ppm) = 7.31 (2H, s, NH_2 , D_2O exchangeable), 7.56-7.65 (2H, m, Ar-H), 7.76 (1H, t, $J = 6$ Hz, Ar-H), 8.00 (1H, s, thiazolyl-H), 8.05 (1H, d, $J = 6.4$ Hz, Ar-H), 8.15 (1H, d, $J = 7.2$ Hz, Ar-H), 8.31 (1H, d, $J = 6.8$ Hz, Ar-H), 9.21 (1H, s, coumarinyl-H). ^{13}C NMR (100 MHz, $\text{DMSO-}d_6$) δ (ppm) = 108.8, 113.0, 114.0, 116.4, 119.5, 121.5, 126.1, 128.6, 129.1, 130.0, 132.7, 133.5, 151.7, 158.7, 167.6. FT-IR (KBr) ν (cm^{-1}) = 3369, 3043, 1730, 1710, 1680, 1620, 1597, 1550, 1462, 1392, 1344, 1263, 1219, 1165, 1029, 970. UV-visible (acetonitrile, 50 μM) = λ_{max} (nm) 383 ($n-\pi^*$).

2.3.2. General procedure for synthesis of probes 3a-3b

A solution of salicylaldehyde (0.305 gm, 2.5 mmol) in ethanol (5 mL) was added slowly in dropwise manner over 15 minutes to the amino-thiazolyl derivative **2a** (0.488 gm, 2.0 mmol) or **2b** (0.588 gm, 2.0 mmol) dissolved in 30 mL ethanol under reflux condition. Then the solution was allowed to reflux for 8 h with stirring till complete precipitation is formed. The precipitate obtained was then filtered under hot condition and washed with hot ethanol for several times to remove the unreacted salicylaldehyde. The solid product obtained was dried in vacuum to get the pure compound **3a** or **3b** as yellow colour powder in quantitative yields (**3a** = 92 %, **3b** = 85 %).

3-(2-(2-hydroxybenzylideneamino)thiazol-4-yl)-2H-chromen-2-one (3a)

M.P. = 230 $^{\circ}\text{C}$. ^1H NMR (400 MHz, $\text{DMSO-}d_6$) δ (ppm) = 7.00 (2H, m, Ar-H), 7.40 (1H, t, $J = 8$ Hz, Ar-H), 7.47 (2H, m, Ar-H), 7.64 (1H, t, $J = 8$ Hz, Ar-H), 7.90 (1H, d, $J = 8.0$ Hz, Ar-H), 7.97 (1H, d, $J = 8$ Hz, Ar-H), 8.37 (1H, s, coumarinyl-H), 8.88 (1H, s, thiazolyl-H), 9.38 (1H, s, aldimine-H), 11.53 (1H, s, Ar-OH, D_2O exchangeable). ^{13}C NMR (100 MHz, $\text{DMSO-}d_6$) δ (ppm) = 115.9, 116.9, 119.1, 119.5, 119.8, 120.0, 124.8, 129.1, 131.1, 132.1, 135.2, 139.8, 145.7, 152.6, 158.8, 160.3, 164.3, 170.4. FT-IR (KBr) ν (cm^{-1}) = 3132, 3041, 1735 ($>\text{C}=\text{O}$), 1724, 1625, 1610 ($>\text{C}=\text{N}$), 1571, 1508, 1475, 1367, 1288, 1170, 1095, 1016, 904. UV-visible

(acetonitrile, 50 μM) = $\lambda_{\text{max}}(\text{nm})$ 346, 378 ($n-\pi^*$). Fluorescence emission (acetonitrile, 50 μM) $\lambda_{\text{em}} = 535$ nm at λ_{ex} 375 nm.

2-(2-(2-hydroxybenzylideneamino)thiazol-4-yl)-3H-benzo[f]chromen-3-one (3b)

M.P. = 285 $^{\circ}\text{C}$. ^1H NMR (400 MHz, $\text{DMSO}-d_6$) δ (ppm) = 6.96 (2H, br d, Ar-H), 7.28 (2H, br s, Ar-H), 7.51-7.79 (3H, m, Ar-H), 8.08-8.32 (3H, m, Ar-H), 9.22 (1H, s, coumarinyl-H), 10.26 (1H, s, thiazolyl-H), 10.72 (1H, s, aldimine-H), 11.65 (1H, s, Ar-OH, D_2O exchangeable). ^{13}C NMR (100 MHz, $\text{DMSO}-d_6$) δ (ppm) = 108.8, 113.2, 116.4, 117.2, 119.5, 119.7, 121.5, 122.3, 126.1, 128.5, 128.6, 129.1, 129.2, 130.0, 132.6, 133.4, 136.4, 143.5, 151.7, 158.7, 160.7, 167.6. FT-IR (KBr) ν (cm^{-1}) = 3498, 3441, 1720 ($>\text{C}=\text{O}$), 1602 ($>\text{C}=\text{N}$), 1562, 1502, 1282, 1211, 1192, 1170, 1151, 1076, 908. UV-visible (acetonitrile, 50 μM) = $\lambda_{\text{max}}(\text{nm})$ 386 ($n-\pi^*$). Fluorescence emission (acetonitrile, 50 μM) $\lambda_{\text{em}} = 540$ nm at λ_{ex} 375 nm.

2.4. UV-visible study of the probes with anions

For UV-visible experiments 50 μM concentration of **3a** and **3b** were prepared from their stock solutions (1 mM). Anion selectivity study was conducted by addition of 10 equivalents of various anions individually to 50 μM solution of **3a** and **3b** in organic and aqueous medium and measuring their absorbance values from 270 to 700 nm. UV-visible titration experiments were carried by gradual addition of various equivalents of the respective anion through a micro pipette to a 2 mL (50 μM) solution of **3a** and **3b** in a cuvette in organic and aqueous medium and the absorption spectra were recorded.

2.5. Fluorescence study of the probes with anions

For fluorescence measurements 50 μM concentration of **3a** and **3b** were prepared from their stock solutions (1 mM). The emission spectra were recorded from 390 to 650 nm with a slit-width of 5 mm by exciting the probes at 375 nm throughout all the fluorescence spectral analysis. Anion selectivity study was conducted by addition of 10 equivalents of various anions individually to 50 μM solution of **3a** and **3b** in organic and aqueous medium. Fluorescence titration experiments were carried by gradual addition of various equivalents of the respective anion through a micro pipette to a 2 mL (50 μM) solution of **3a** and **3b** in a cuvette in organic and aqueous medium and the emission spectra were recorded.

2.6. NMR titration experiments

A 5 mM solution of probe **3a** was prepared in DMSO-*d*₆. To a 0.5 mL of probe solution, various equivalents of tetrabutylammonium fluoride (from a stock of 10 mM in DMSO-*d*₆) and potassium cyanide (from a stock of 10 mM in DMSO-*d*₆ or 10 mM in water) were added to an NMR tube through a micro pipette and the spectra were recorded.

2.7. Computational calculations

All quantum chemical calculations were carried out by using the TURBOMOLE program suite [53]. The single point geometry optimizations and frontier molecular orbital properties of the concerned molecules at acetonitrile solvent phase ($\epsilon = 37.5$) were carried out by employing Density Functional Theory [54, 55] at B3LYP[56]/TZVP[57] level of theory taking the advantage of the RI [58, 59] approximation which yields an acceleration by a factor of 5–10 [60].

3. Results and Discussion:

3.1. Synthesis and characterization of probe **3a-b**

The synthesis of probes **3a-b** could be achieved through facile synthetic protocols as depicted in Scheme 1 and Figure S1. Reaction of **1a-b** with thiourea in presence of sodium acetate in ethanol at 60 °C afforded the thiazolyl-coumarin derivatives **2a-b** [52]. Condensation reaction of **2a-b** with salicylaldehyde in ethanol under reflux condition produced the thiazolyl-coumarin-salicylidene probes **3a-b** in quantitative yields. The spectroscopic analysis of **2a-b** and **3a-b** were consistent with their indicated structures (Figures S2-S13, Supporting information). For instance the ¹H NMR spectra of **3a** exhibited a singlet at a most downfield region of 11.53 ppm which could be attributed to phenolic –OH proton that disappeared upon addition of D₂O. In probe **3b** the corresponding –OH signal disappeared at 11.65 ppm on D₂O addition. **3a** exhibited three D₂O non-exchangeable singlets at 9.38, 8.88 and 8.37 ppm integrating to one proton each which could be assigned to aldimine (–CH=N–), thiazolyl (–CH=) and coumarinyl (–CH=) protons respectively while probe **3b** correspondingly showed the same set of D₂O non-exchangeable singlets at 10.72, 10.26 and 9.22 ppm. The aromatic proton signals of **3a** and **3b** appeared in the range of 6.96–8.32 ppm. The ¹³C NMR signals at 170.4 and 167.6 ppm respectively in **3a** and **3b** could be attributed to the thiazolyl (–S–CH=N–) carbon while the signals at 160.3 and 160.7 could be correspondingly assigned to the aldimine (–CH=N–) carbon in **3a** and **3b** which evident

the formation of thiazolyl-coumarin conjugated salicylidene probes. The FT-IR spectrum exhibited sharp peaks at 1735 and 1610 cm^{-1} in **3a** and 1720 and 1602 cm^{-1} in **3b** which could be attributed to the stretching frequencies of C=O and C=N bonds respectively.

3.2. Anion interaction study of probe 3a-b by colorimetric analysis in organic and aqueous medium

The visual response of probe **3a-b** against various anions (such as F^- , Cl^- , Br^- , I^- , H_2PO_4^- , HSO_4^- , AcO^- and CN^-) was first monitored through colorimetric analysis in organic (acetonitrile, ACN) medium. It was found that the probe **3a** exhibited a prominent and instant colour change from colourless to deep red only with fluoride ions while no significant colour response was observed on treatment with Cl^- , Br^- , I^- , H_2PO_4^- and HSO_4^- ions under analogous condition (Figure 1a). Similarly probe **3b** showed a prominent colour change from colourless to red only in presence of fluoride ions (Figure S14, Supporting information). On the other hand interaction of **3a** and **3b** with AcO^- and CN^- ions exhibited a faint colour change in comparison to that observed with fluoride ions (Figure 1 and Figure S14, Supporting information). When a similar set of colorimetric analysis was carried out in aqueous medium (H_2O -ACN, 1:1 v/v), it was interesting to note that the probe **3a** exhibited a instantaneous colour change from colourless to deep yellow only with cyanide ions while no optical response was observed on treatment with F^- , Cl^- , Br^- , I^- , H_2PO_4^- , HSO_4^- , AcO^- ions as shown in Figure 1b.

Moreover the colorimetric analysis of the interaction of **3a** with CN^- ions was tested in different percentage of aqueous acetonitrile mixture ranging from 95/5 to 5/95 (ACN- H_2O v/v) which exhibited that the detection of cyanide ions could be possible through visual colour change in aqueous medium as high as 50% by volume of water (Figure S15, Supporting information). However the probe **3b** exhibited poor solubility in aqueous acetonitrile mixture even at 5% by volume of water and therefore precipitated out from the mixture solvent. As a result probe **3b** could not be employed for colorimetric testing of anions in aqueous medium.

3.3. UV-visible study of probe 3a-b with anions in organic and aqueous medium

Based on the results obtained from the colorimetric analysis, UV-visible spectroscopic investigations of **3a-b** upon interaction with fluoride and cyanide ions were performed at 50 μM concentration. Addition of fluoride ions to **3a** and **3b** in organic medium exhibited a newly

developed longer wavelength absorption peak at 491 and 494 nm respectively while no change was observed in the UV-visible spectrum of **3a-b** upon addition of Cl^- , Br^- , I^- , H_2PO_4^- and HSO_4^- ions as depicted in Figure 2a and Figure S16, Supporting information. On the other hand a similar absorption band at 491 and 494 nm with low intensity was observed in the UV-visible spectrum of **3a** and **3b** respectively upon addition of acetate and cyanide ions, which indicated poor binding nature of these anions in comparison to fluoride ions (Figure 2a and Figure S16, Supporting information). Conversely, addition of F^- , Cl^- , Br^- , I^- , H_2PO_4^- , HSO_4^- , AcO^- and CN^- ions to **3a** in aqueous medium exhibited a longer wavelength absorption peak at 460 nm only in the presence of cyanide ions as shown in Figure 2b.

It was further observed that, gradual addition of a standard solution of fluoride ions (TBAF) to 50 μM solution of **3a** and **3b** in organic medium resulted in progressive increase in the absorption peak centred at 491 and 494 nm respectively with simultaneous decrease in the absorption band at 378 and 386 nm in the UV-visible spectra with the appearance of an isobestic point at 421 and 428 nm respectively (Figure 3 and Figure S17, Supporting information). When the concentration of fluoride addition approached to one equivalent with respect to **3a** or **3b**, a colour change from colourless to reddish was observed in the probe solution and this colour became deeper on further addition of fluoride ions with concomitant increase in the intensity of absorption band at 491 or 494 nm. The observed colorimetric changes in probe solutions reached its limiting value on addition of two equivalents of fluoride ions.

A more detail analysis of the UV-visible titration results of probe **3a** and **3b** indicates that the limiting value in the absorption maxima centered at 491 and 494 nm was attained after two equivalents of F^- ions. This can be accounted for by hypothesizing that the initial addition of one equivalent of F^- ion establishes a hydrogen bond interaction with OH proton of the probe through 1:1 hydrogen bonded adduct formation. On further addition of fluoride ions beyond one equivalent to the 1:1 complex, the first hydrogen bonded fluoride ion cooperates to bind the second fluoride ion which led to the formation of 1:2 hydrogen bonded adduct between the probe and fluoride ions and subsequently undergoes deprotonation just beyond two equivalent addition of fluoride ions to form a more stable bifluoride $[\text{HF}_2]^-$ species [61, 62] with highest calculated hydrogen bond energy (39 kcal mol⁻¹) [63] as shown in Scheme 2. Experimental observations indicate that the appearance of new absorption band at higher wavelengths (491 nm in **3a** or 494 nm in **3b**) during probe-fluoride interaction could be either due to the formation of hydrogen

bonds with the phenolic –OH or its deprotonation by fluoride ions which results in a visual colour change possibly through efficient intramolecular charge transfer (ICT) [48].

UV-visible titration experiments of probe **3a** and **3b** with cyanide ion (KCN in DMSO) in organic medium (50 μ M) exhibited a concurrent increase in the absorption peak at 491 and 494 nm respectively, however, with lesser intensity as shown in Figure 4a and Figure S18, Supporting information. On the other hand, titration of cyanide ion (KCN in water) with 50 μ M solution of **3a** in aqueous medium showed gradual increase of an absorption peak at 460 nm with a visual colour change from colourless to yellow in the probe solution (Figure 4b). Analysis of the titration profiles of cyanide ion with **3a** in organic and aqueous medium indicates that the intensity of the absorption peaks at 491 and 460 nm respectively reached the limiting value beyond two equivalents of cyanide addition. Similarly the titration experiments of **3a** and **3b** with acetate ion (TBAACO) in organic medium showed analogous results as that of cyanide ion with a gradual increase in the absorption peak at 491 and 494 nm respectively as shown in Figure S19-S20, Supporting information.

The binding characteristics of probe **3a** and **3b** with fluoride, acetate and cyanide ions was quantitatively analysed by Job's continuous variation plots which revealed a maximum absorbance at 0.33 mole fraction of probe to indicate a 1:2 binding stoichiometry for the interaction of **3a** or **3b** with fluoride and cyanide ions (Figure 5-6). However, a maximum absorbance at 0.5 mole fraction of probe was observed in presence of acetate ions which indicated a 1:1 binding stoichiometry between the probe and acetate ions (Figure S21, Supporting information).

The apparent binding constants (K) of **3a** and **3b** in the presence of fluoride, acetate and cyanide ions were determined from the UV-visible titration data using nonlinear regression analysis and depicted in Figure S22 (Inset of Figure 4a and 4b). From the binding constant values it was clearly understood that the probes have more binding affinity for fluoride ion (for **3a**, $K = 2.0 \times 10^5$ and **3b**, $K = 1.2 \times 10^5 \text{ M}^{-1}$) than acetate and cyanide ions in organic medium while in aqueous medium probe **3a** showed high binding affinity towards the cyanide ions ($K = 1.83 \times 10^5 \text{ M}^{-1}$) than fluoride and acetate ions. This could be possible due to different hydrogen bonding abilities of fluoride, acetate and cyanide ions in organic and aqueous medium. Moreover the comparatively higher nucleophilicity and lower hydration energy for the cyanide ion ($\Delta H_{\text{hyd}} =$

–67 kJ/ mol) than that of the fluoride ($\Delta H_{\text{hyd}} = -505$ kJ/mol) and acetate ion ($\Delta H_{\text{hyd}} = -375$ kJ/mol) explains the selectivity of cyanide ion towards probe **3a** in aqueous medium [50, 64, 65].

3.4. Fluorescence study of probe **3a-b** with anions in organic and aqueous medium

Further investigations of the binding mode of probe **3a** and **3b** with the anionic species was carried out by fluorescence spectroscopic technique in a 50 μM probe solution both in organic and aqueous medium. The emission spectra were recorded from 390 to 650 nm with a slit-width of 5 nm by exciting the probes at 375 nm throughout all the fluorescence spectral analysis. It was observed that, addition of 10 equivalents of various anions such as F^- , Cl^- , Br^- , I^- , H_2PO_4^- , HSO_4^- , AcO^- (as TBA salts) and CN^- (as KCN) to **3a** in organic medium resulted in an intense emission peak at 484 nm only in presence of fluoride ions (Figure S23, Supporting information). In a similar experiment, addition of various anions to 50 μM probe solution in aqueous medium showed a significant increase in the fluorescence intensity at 506 nm only in the presence of cyanide ions (Figure S24, Supporting information). This indicated that the probe is quite selective and specific towards CN^- ion in aqueous medium.

A more detail understanding about the binding mode of probe **3a** with anions were achieved through fluorescence titration experiments by adding various equivalents of anions to a 50 μM probe solution in organic and in aqueous medium. It was observed that in absence of anions the probe exhibited an emission peak at 535 nm with a very low intensity in organic medium. On gradual addition of fluoride ions from 0 to 5 equivalents, a hypsochromically shifted ($\Delta\lambda = 51$ nm) peak was correspondingly increased at a wavelength of 484 nm that became saturated beyond two equivalents of fluoride ions with a fluorescence ‘turn on’ behavior through enhancement in fluorescence intensity by 150-folds (Figure 7).

A similar titration experiment of the probe **3a** in aqueous medium by incremental addition of CN^- ions showed a 37-folds increase in the fluorescence intensity of a hypsochromically shifted ($\Delta\lambda = 29\text{nm}$) emission peak at 506 nm up to the addition of two equivalents of cyanide ion (Figure 8).

These interpretation can be figure out from earlier reports which recommended that fluorescence “turn-on” is a result of intramolecular charge transfer because of anion-probe interactions which may suppress the $n-\pi^*$ transitions to facilitate the $\pi-\pi^*$ transitions mostly responsible for the emissive behavior of the probe [66]. The fluorescence ‘turn on’ behavior exhibited by probe **3a** is highly selective for fluoride ions in organic medium and cyanide ions in aqueous medium which were in good agreement with the UV-visible experiments.

On the other hand addition of 10 equivalents of various anions such as F^- , Cl^- , Br^- , I^- , $H_2PO_4^-$, HSO_4^- , AcO^- and CN^- to **3b** in organic medium resulted in an intense emission peak at 490 nm only in presence of fluoride ions. In absence of anions the probe **3b** exhibited a weak emission peak at 540 nm in organic medium. Titration of fluoride ions from 0 to 5 equivalents with **3b** exhibited a gradual increase of a hypsochromically shifted ($\Delta\lambda = 50\text{nm}$) emission peak at 490 nm that became saturated beyond two equivalents of fluoride ions with an enhancement in the fluorescence intensity by 160-folds as shown in Figure 9.

The fluorescent colour changes observed for the probe **3a** and **3b** upon interaction with the anionic species is shown in Figure 10 and Figure S25, Supporting information. This indicated that both the probes exhibited a more prominent fluorescence colour change from colourless to yellow in presence of fluoride ions. The selectivity of the fluoride ion in organic medium in comparison to other anions for emission enhancement in **3a** and **3b** may be ascribed to its greater hydrogen bonding and deprotonation ability. This finding in our case is worthy to note as it exhibits a fluorescence “turn on” behavior in comparison to earlier reports [28-30, 67-74] which showed fluorescence quenching rather than enhancement on fluoride binding. On the other hand **3a** exhibited a significant fluorescence change from colourless to green selectively with cyanide ions in comparison to other anions in aqueous medium (Figure 10).

3.5. Fluorescent detection limits of probe 3a towards fluoride and cyanide ions

The values of limit of detection (LOD) and limit of quantification (LOQ) of probes **3a** and **3b** with F^- and CN^- ion were determined from the fluorescence titration experiments in organic and aqueous medium. From the fluorescence measurements, the LOD and LOQ of the emission changes were calculated on the basis of $3(\sigma/K)$ and $10(\sigma/K)$ respectively where (σ) and (K) represents the calculated standard deviation of intercepts and the slope of the emission calibration curve respectively (Figure S26, Supporting information). The LOD values clearly

indicate that both **3a** (LOD = 0.72 μM ; LOQ = 2.4 μM) and **3b** (LOD = 0.46 μM ; LOQ = 1.5 μM) possesses a high level of sensitivity at submicromolar concentration of fluoride ions in organic medium while probe **3a** is selectively sensitive for the detection of cyanide ions at micro molar concentration (LOD = 2.7 μM ; LOQ = 8.9 μM) in aqueous environment. Moreover the detection limits of probes **3a** and **3b** are within range of the permissible limit of 1.5 mg/L and 0.07 mg/L set by World Health Organization (WHO) respectively for fluoride and cyanide ion concentrations in drinking water [75, 76]. The binding constants, fluorescence enhancement ratios and limit of detection (LOD) values of probe **3a** and **3b** towards fluoride and cyanide ions were found to be higher than the salicylidine based fluoride and cyanide sensors reported recently [39, 43-45, 48, 50].

3.6. pH study of probe **3a** with cyanide ions in aqueous medium

We have also investigated the effect of pH on the absorption and emission response of probe **3a** and its interaction with CN^- ions in a series of solutions with pH values ranging from 1 to 13 in aqueous medium (Figure S27, Supporting information). From the UV-visible and fluorescence measurements it was observed that the probe **3a** exhibits a stable response in the pH range of 3 to 9. Below pH 3 and above pH 9 the intensity of absorption and emission maxima of the probe is altered possibly because of protonation and deprotonation of the phenolic $-\text{OH}$ group in a highly acidic and basic pH respectively. Based on this observation we have examined the detection response of **3a** towards CN^- ion in the pH range of 4 to 9 by UV-visible and fluorescence analysis in aqueous medium as depicted in Figure 12.

Addition of 10 equivalents of CN^- ion to the solution of **3a** resulted in a colour change from colourless to yellow and increase in the absorption band at 460 nm over the tested pH range 4 to 9. Similarly an intense and stable fluorescence of **3a**- CN^- complex at 506 nm was observed in the pH range of 4 to 9. These results warrant the application of probe **3a** for the colorimetric and fluorometric detection of cyanide ions over a wide pH range of 4.0 to 9.0.

3.7. ^1H NMR study of probe **3a** with fluoride and cyanide ions

To further study the nature of the interaction between probe **3a** with fluoride and cyanide ions, ^1H NMR titration experiments were conducted in DMSO-d_6 at 5 mM concentration of the probe solution. Figure 13 shows the ^1H NMR titration spectra of **3a** in the absence and presence of various equivalents of fluoride ions. For instance, the ^1H NMR spectrum of probe **3a**, in the absence of fluoride ions exhibited four singlets at δ 11.53, 9.38, 8.88, 8.37 ppm corresponding to

one proton each which can be attributed to hydroxyl (-OH) group and proton numbers H5, H6 and H7 respectively. Addition of 0.5 equivalent of fluoride ion resulted in a colour change of the solution from pale yellow to reddish with a significant change in the NMR spectrum. The -OH signal at δ 11.53 ppm became broaden while the singlets at 9.38, 8.88, 8.37 ppm corresponding to protons H5, H6 and H7 exhibited an upfield shift. On the other hand the aromatic signals at δ 7.92, 7.49 and 7.02 ppm corresponding to protons H4, H2, H1 and H3 respectively exhibited a significant upfield shift ranging from $\Delta\delta$ 0.36-1.11 ppm by gradual addition of fluoride ions up to 3 equivalents. Further addition of fluoride ions beyond 3 equivalents did not exhibit any shift in the resonance values of the proton signals of **3a**. However, the aromatic signals of the coumarin unit at δ 7.99, 7.66 and 7.44 ppm corresponding to protons H8, H9, H10 respectively remain unaltered during the entire titration experiments. These observations indicates that addition of 0.5 equivalent of fluoride ions initially form a hydrogen bonded complex with the probe at the -OH group resulting in broadening of the signal at 11.53 ppm which subsequently disappeared upon the addition of higher equivalents of F⁻ ions possibly due to deprotonation in the -OH group. This has been confirmed by the appearance of a triplet signal at around 16 ppm due to the formation of HF₂⁻ species beyond two equivalents of fluoride ions through deprotonation as proposed in Scheme 2.

This process of interaction of fluoride ion with probe **3a** by the initial hydrogen bond formation and subsequent deprotonation was further confirmed from the gradual upfield shift of the aromatic signals corresponding to the salicylidene ring possibly due to increase in electron density through charge transfer. For example, the doublet signal at 7.92 corresponding to H4 proton exhibited a gradual upfield shift of 0.36 ppm by the addition of 3 equivalents of F⁻ ions. Interestingly the merge signal at 7.49 corresponding to H11 and H2 protons exhibited a gradual upfield shift only in H2 signal upon the addition of various equivalents of fluoride ions while the H11 signal of the coumarin unit remains unchanged which indicates the possible delocalization of the electron density around the salicylidene ring on deprotonation. Similarly the merge signal at 7.02 ppm corresponding to H1 and H3 of the salicylidene unit showed an upfield shift of $\Delta\delta$ 0.85 and 1.11 ppm respectively and appeared as a doublet and triplet signal beyond 3 equivalents of fluoride addition.

Cyanide ions are well-known to interact with a molecular system in various ways such as through hydrogen bond formation and/or by nucleophilic addition reaction at electrophilic carbon centers [7, 31]. Therefore, in order to get a better understanding of interaction of cyanide ions with probe **3a**, ¹H NMR titration experiments were conducted and showed in Figure 14.

Like the fluoride ions, the addition of various equivalents of cyanide ions to a 5 mM solution of **3a** in DMSO- d_6 showed a colour change from pale yellow to reddish; however it showed a completely different pattern of titration spectra in comparison to that of fluoride ions. For example, addition of 0.5 equivalent of cyanide ion to **3a** showed broadening of the -OH signal at 11.53 ppm (data not shown) and also exhibited six prominent singlets in the NMR spectrum along with a number of splitted signals in the upfield region (Figure 14). Further addition of cyanide ions up to 5 equivalents gradually simplifies the spectral pattern and beyond the addition of 3 equivalents it shows an analogous shift in protons H1, H2 and H3 as that of the fluoride ions. However the upfield shifts exhibited by the aromatic protons H1, H2 and H3 of the salicylidene unit are less than that observed in case of fluoride ions. On the other hand, the singlet protons H5, H6 and H7 exhibited a more pronounced upfield shifts beyond 3 equivalents of cyanide addition in comparison to fluoride ions. These observations indicate that the interaction of **3a** with cyanide ions is reasonably different than that with fluoride ions.

The appearance of significantly different NMR spectrum of **3a** at 0.5 equivalent of cyanide ion in comparison to fluoride ion indicates that cyanide ions could possibly interact with the probe not only through hydrogen bond formation at the -OH group but also interact by nucleophilic addition reaction at the azomethine ($-CH^5=N-$) and coumarinyl ($-CH^7=C<$) carbon centers of the probe as evidenced in earlier reports [45, 77-78]. Therefore at lower concentration of cyanide ions (upto 1 eqvt.) there is possibility of existence of multiple species such as hydrogen bonded adduct (A) and nucleophilic adducts (B) and (C) along with a combination of A, B and C species which resulted in a more complex spectral pattern than that observed in fluoride ion at lower concentration (Scheme 3).

The formation of probe-cyanide hydrogen bonded adduct (equilibrated between species A and B) has been confirmed by the analogous upfield shifts exhibited by the salicylidene aromatic signals H1, H2 and H3 through gradual addition of CN^- ions similar to the case of fluoride ions. However the magnitude of upfield shift of protons H1, H2 and H3 observed in the presence of excess of cyanide ions (5 eqvt.) ($\Delta\delta_{H1}=0.58$, $\Delta\delta_{H2}=0.54$, $\Delta\delta_{H3}=0.74$ in ppm) are found to be smaller than that observed in the presence of fluoride ions ($\Delta\delta_{H1}=0.87$, $\Delta\delta_{H2}=0.59$, $\Delta\delta_{H3}=1.11$ in ppm). This clearly indicates that the flow of electron density from the -OH group towards the salicylidene aromatic ring through charge transfer is trivial in presence of cyanide ions than that observed with fluoride ions. This is possibly because of poor basicity of cyanide ion which can strongly polarize the H-O bond through hydrogen bonding but could not induced a complete deprotonation of -OH group even at higher concentration as observed in presence of excess

fluoride ions. This result was in good agreement with the colorimetric and UV-visible spectroscopic studies which showed a faint colour change and lower intensity absorption band in probe **3a** with cyanide ions in comparison to fluoride ions in organic medium. On the other hand the formation of cyanide nucleophilic addition products (B) and (C) (Scheme 3) have been confirmed by appearance of significant upfield shift in the signal of azomethine proton (H5) and coumarinyl proton (H7) by $\Delta\delta$ 1.77 and 2.41 ppm respectively. Moreover the upfield shift exhibited by salicylidene aromatic proton (H4) is more prominent in presence of cyanide ion ($\Delta\delta_{H4}=0.76$ in ppm) than that observed with fluoride ion ($\Delta\delta_{H4}=0.36$ in ppm). This indicates that a CN group is attached at the azomethine carbon through nucleophilic addition process which resulted in a more upfield shift of proton H4 possibly due to shielding effect of CN group. Finally at higher concentration of cyanide ions beyond 2 equivalents the NMR spectrum of probe **3a** became simpler possibly due to the formation of one species (D) as proposed in Scheme 3.

In order to understand the binding process of cyanide ions with probe **3a** in aqueous medium, we have conducted the ^1H NMR titration experiments with gradual addition of various equivalents of CN^- ion from an aqueous stock solution (10 mM KCN in water) to a 5 mM probe solution in DMSO-d_6 . It was observed that a colour change from pale yellow to deep yellow was obtained with gradual upfield shifts in proton signals of H1, H2, H3 and H4 similar to that observed by addition of cyanide ions in pure DMSO medium. However at the saturation point beyond two equivalent additions of CN^- ions from aqueous solution, the magnitude of upfield shifts exhibited by salicylidene protons H1, H2, H3 and H4 are found to be smaller than that observed in pure DMSO medium (Figure S28, Supporting information). This indicates that the charge transfer from $-\text{OH}$ group towards the salicylidene ring is weaker in water medium than in pure DMSO possibly because of hydration of probe-cyanide complex. This was further supported from the colorimetric and UV-visible experiments which showed a visible colour change from colourless to yellow in the probe solution with an absorption maxima at 460 nm by addition of cyanide ions in aqueous medium.

3.8. Computational analysis of probe **3a** with fluoride and cyanide ions

Further understanding of the photophysical properties of probe **3a** and its interaction with fluoride and cyanide ions were carried out by theoretical models using quantum chemical calculations. The obtained optimized structures of probe **3a** and its complexes with fluoride and cyanide ions were visualized by using Gauss view programme and are shown in Figure 15.

The optimized molecular geometry of **3a** demonstrates that the N-atom of the azomethine group interacts with phenolic OH through a six-member hydrogen bonding network with bond length of 1.30 Å of O-H \cdots N type with heavy atom distance, 2.40 Å. Further information about the mechanism of interaction of **3a** with the anions was obtained from the typical transition energy diagram for the highest occupied molecular orbital (HOMO) and the lowest unoccupied molecular orbital (LUMO) of the probe **3a** along with its resultant complexes with fluoride and cyanide ions as shown in Figure 16. The total energy of **3a**+F $^-$ (-42567.95 eV), **3a**+CN $^-$ at -OH (-42375.91 eV), and **3a**+CN $^-$ at -CH 5 =N (-42376.46 eV), **3a**+CN $^-$ at -CH 7 =C (-42375.54 eV) **3a**+2CN $^-$ at -CH 5 =N and -CH 7 =C (-44905.39 eV) optimized complexes in DFT were found to be lower than the total energy of the free probe (-39846.84 eV) which indicates the greater stability of the complexes. However the calculated energy of the HOMO and LUMO levels of the fluoride and cyanide complexes was found to be increased from that of the HOMO and LUMO energies of the free probe (Figure 16) which can be attributed due to the distortion in the molecular geometry and disruption in the six-member hydrogen bonding network in **3a** during the complexation process. On the other hand the results of the quantum chemical calculations further indicates that the difference in the energy gap between the HOMO and LUMO of probe **3a** was found to be larger than that of the complexes. This result was in good agreement with the red shifts observed in the absorption spectra of probe **3a** upon the addition of F $^-$ and CN $^-$ ions.

It was interesting to note that the total energy of three types of 1:1 cyanide complexes with **3a** (i.e. product A, B and C of Scheme 3) was found to be very close to each other whereas 1:2 cyanide complex (product D) exhibited a lowering in total energy and hence attain a greater stability (Figure 15). This indicates that at lower concentration of cyanide ions (upto 1 eqvt.) there is a strong possibility of formation of all the three products A, B and C in solution phase while at higher concentration it led to the formation of single product D due to its enhance stability. This result was well concordant with the ^1H NMR observations which showed the formation of A, B and C complexes at lower concentration of cyanide addition while at higher concentrations beyond 2 equivalents it ultimately resulted in the formation of D type complex with **3a**.

3.9. Practical applications of probe **3a**

Considering the important applications of cyanide in industry [79], the detection of cyanide in natural environment by visual and fluorescence method in aqueous medium by probe **3a** has been investigated. Moreover to verify the possible interference of other components and ions

present in real samples in the detection of cyanide ion, we have taken the town supply tap water as the medium of analysis. Different amounts of potassium cyanide were added to tap water in order to make the final concentrations of cyanide ion between 2 to 100 μM . A 50 μM probe solution was prepared in aqueous medium (H_2O -Acetonitrile 1:1 v/v) and different concentrations of cyanide ion in tap water were added to the probe solution. The observed visual and fluorescence colour change was depicted in Figure 17 which indicated that the probe could be applied for the detection of cyanide ion at micromolar range in environmental samples.

4. Conclusions

In summary, two chromofluorescent salicylidine probes **3a** and **3b** functionalized with thiazolyl-coumarin derivatives have been synthesized through simple condensation reactions in quantitative yields. Both **3a** and **3b** selectively recognizes fluoride ions among the other anions through a distinct visual colour change from colourless to red with the appearance of a new longer wavelength absorption peak at 491 and 494 nm respectively in their UV-visible spectra in organic medium. Interestingly probe **3a** could optically discriminate the presence of fluoride and cyanide ion in organic and aqueous medium respectively through a significant colorimetric change and fluorescence “turn-on” in the probe solution. Job’s plot analysis revealed a 1:2 binding stoichiometry between the probes and fluoride or cyanide ion while a 1:1 binding stoichiometry was observed with acetate ion. ^1H NMR titration experiments of **3a** with fluoride ions further revealed a step wise binding process of F^- ion with the probe and subsequent deprotonation of phenolic -OH group beyond two equivalents of fluoride ions. On the other hand interaction of cyanide ion with probe **3a** by hydrogen bond formation as well as nucleophilic addition reactions were well established from the ^1H NMR titration experiments of **3a** with cyanide ions in organic and aqueous medium. The results obtained from the proton NMR titration experiments were concurred with the colorimetric and UV-visible observations. Moreover the results of the quantum chemical calculations of probe **3a** in the presence of fluoride and cyanide ion indicates a decrease in total energy and lowering of HOMO-LUMO energy gap in probe **3a** upon interaction with the anionic species which were in good agreement with the experimental data. The detection limits of probe **3a** and **3b** were found to be in submicromolar and micromolar concentrations of fluoride and cyanide ions in organic and aqueous medium respectively which indicated their high level of sensitivity. Moreover the pH studies suggested that **3a** could detect the cyanide ions over a wide pH range of 4.0 to 9.0 *via* a colorimetric and fluorescence response. Taken together, the newly synthesized probes **3a** and **3b**

are extremely good candidates for sensing fluoride ion in organic medium while probe **3a** could be used for the detection of cyanide ions in aqueous medium through visual colour change and fluorescence enhancement.

Acknowledgements

S.N.S gratefully acknowledges the financial assistance received from DST, New Delhi for the Fast-Track project grant (SR/FT/CS-46/2011). S.K.P is thankful to DST and UGC New Delhi for a project assistantship and BSR fellowship respectively. Authors are thankful to Central Instruments Facility, NIT Rourkela and IIT Guwahati for recording the NMR spectra and also to the Computational Facility at NIST Berhampur for quantum chemical calculations. The financial assistance received from UGC and DST New Delhi under the DRS and FIST grant respectively to School of Chemistry is gratefully acknowledged. We are thankful to Dr. H. Chakraborty for his useful suggestions towards the improvement of this manuscript.

Appendix A. Supplementary data

Supplementary data associated with this article can be found, in the online version, at

References

- [1] N. Busschaert, C. Caltagirone, W. Van Rossom, P. A. Gale, Applications of Supramolecular Anion Recognition, *Chem. Rev.* 115 (2015) 8038-8155.
- [2] X. Lou, D. Ou, Q. Li, Z. Li, An indirect approach for anion detection: the displacement strategy and its application, *Chem. Commun.* 48 (2012) 8462–8477.
- [3] C. Caltagirone, P. A. Gale, Anion receptor chemistry: highlights from 2007, *Chem. Soc. Rev.* 38 (2009) 520–563.
- [4] V. Amendola, M. Bonizzoni, D. E. Gomez, L. Fabbrizzi, M. Licchelli, F. Sancenon, A. Taglietti, Some guidelines for the design of anion receptors, *Coord. Chem. Rev.* 250 (2006) 1451–1470.
- [5] A. T. Wright, E. V. Anslyn, Differential receptor arrays and assays for solution-based molecular recognition, *Chem. Soc. Rev.* 35 (2006) 14–28.
- [6] A. Bianchi, K. Bowman-James and E. Garcia-Espana, *Supramolecular Chemistry of Anions*, Wiley-VCH, New York, 1997.
- [7] P. B. Pati, Organic chemodosimeter for cyanide: A nucleophilic approach, *Sens. Actuators, B: Chem.* 222 (2016) 374–390.
- [8] L. Gai, J. Mack, H. Lu, T. Nyokong, Z. Li, N. Kobayashi, Z. Shen, Organosilicon compounds as fluorescent chemosensors for fluoride anion recognition, *Coord. Chem. Rev.* 285 (2015) 24–51.
- [9] M. Cametti, K. Rissanen, Recognition and sensing of fluoride anion, *Chem. Commun.* 20 (2009) 2809–2829.
- [10] M. Kleerekoper, The role of fluoride in the prevention of osteoporosis, *Endocrinol. Metab. Clin. North Am.* 27 (1998) 441–452.
- [11] K. L. Kirk, *Biochemistry of the Halogens and Inorganic Halides*, Plenum Press, New York, 1991.
- [12] J. Hamel, A Review of Acute Cyanide Poisoning With a Treatment Update, *Crit. Care*

- Nurse, 31 (2011) 72–82.
- [13] K.W. Kulig, Cyanide Toxicity, U. S. Department of Health and Human Services, Atlanta, GA, 1991.
- [14] A. Dhillon, M. Nairb, D. Kumar, Analytical methods for determination and sensing of fluoride in biotic and abiotic sources: a review, *Anal. Methods*, 8 (2016) 5338-5352.
- [15] J. Tao, P. Zhao, Y. Li, W. Zhao, Y. Xiao, R. Yang, Fabrication of an electrochemical sensor based on spiropyran for sensitive and selective detection of fluoride ion, *Anal. Chim. Acta.* 918 (2016) 97-102.
- [16] P. Aggarwal, S. Singh, S. Awasthi, A. Srivastava, M.L. Singla, Voltammetric Determination of Fluoride Ion Using Galvanostatically Grown Poly(3-hexylthiophene) Film, *Sensors & Transducers*. 137 (2012) 85-94.
- [17] A. Safavi, N. Maleki, H. Shahbaazi. Indirect determination of cyanide ion and hydrogen cyanide by adsorptive stripping voltammetry at a mercury electrode, *Anal. Chim. Acta.* 503 (2004) 213-221.
- [18] T. T. Christison, J. S. Rohrer, Direct determination of free cyanide in drinking water by ion chromatography with pulsed amperometric detection, *J. Chromatogr. A.* 1155 (2007) 31-39.
- [19] D. B. Bhatt, P. R. Bhatt, H. H. Prasad, K. M. Popat, P. S. Anand, Removal of fluoride ion from aqueous bodies by aluminium complexed amino phosphonic acid type resins, *Indian J. Chem. Technol.* 11 (2004) 299-303.
- [20] R. S. Sathish, U. Sujith, G. N. Rao, C. Janardhana, Fluoride ion detection by 8-hydroxyquinoline–Zr(IV)–EDTA complex, *Spectrochim. Acta A Mol. Biomol. Spectrosc.* 65 (2006) 565–570.
- [21] D. Shan, C. Mousty, S. Cosnier, Subnanomolar Cyanide Detection at Polyphenol Oxidase/Clay Biosensors, *Anal. Chem.* 76 (2004) 178–183.
- [22] F. Wang, L. Wang, X. Chen, J. Yoon, Recent progress in the development of fluorometric and colorimetric chemosensors for detection of cyanide ions, *Chem. Soc. Rev.* 43 (2014) 4312-4324.
- [23] Z. Xu, X. Chen, H. N. Kim, J. Yoon, Sensors for the optical detection of cyanide ion, *Chem.*

- Soc. Rev. 39 (2010) 127–137.
- [24] Y. Zhou, J. F. Zhang, J. Yoon, Fluorescence and Colorimetric Chemosensors for Fluoride-Ion Detection, *Chem. Rev.* 114 (2014) 5511-5571.
- [25] R. Martinez-Manez, F. Sancenon, Fluorogenic and Chromogenic Chemosensors and Reagents for Anions, *Chem. Rev.* 103 (2003) 4419-4476.
- [26] L. E. Santos-Figueroa, M.E. Moragues, E. Climent, A. Agostini, R. Martinez-Manez, F. Sancenon, Chromogenic and fluorogenic chemosensors and reagents for anions. A comprehensive review of the years 2010–2011, *Chem. Soc. Rev.* 42 (2013) 3489-3613.
- [27] R. M. Duke, E. B. Veale, F. M. Pfeffer, P. E. Kruger, T. Gunnlaugsson, Colorimetric and fluorescent anion sensors: an overview of recent developments in the use of 1,8-naphthalimide-based chemosensors, *Chem. Soc. Rev.* 39 (2010) 3936-3953.
- [28] A. K. Bhoi, S. K. Das, D. Majhi, P. K. Sahu, A. Nijamudheen, N. Anoop, A. Rahaman, M. Sarkar, Analyte Interactions with a New Ditopic Dansylamide–Nitrobenzoxadiazole Dyad: A Combined Photophysical, NMR, and Theoretical (DFT) Study, *J. Phys. Chem. B.* 118 (2014) 9926–9937.
- [29] A. K. Bhoi, P. K. Sahu, G. Jha, M. Sarkar, Combined photophysical, NMR and theoretical (DFT) study on the interaction of a multicomponent system in the absence and presence of different biologically and environmentally important ions, *RSC Adv.* 5 (2015) 61258–61269.
- [30] V. Mohan, A. Nijamudheen, S. K. Das, P. K. Sahu, U. P. Kar, A. Rahaman, M. Sarkar, Ion Interactions with a New Ditopic Naphthalimide-Based Receptor: A Photophysical, NMR and Theoretical (DFT) Study, *Chem. Phys. Chem.* 13 (2012) 3882-3892.
- [31] M. E. Jun, B. Roy, K. H. Ahn, “Turn-on” fluorescent sensing with “reactive” probes, *Chem. Commun.* 47 (2011) 7583-7601.
- [32] M. K. Salomón-Flores, I. J. Bazany-Rodríguez, D. Martínez-Otero, M. A. García-Eleno, J. J. Guerra-García, D. Morales-Morales, A. Dorazco-González, Bifunctional colorimetric chemosensing of fluoride and cyanide ions by nickel-POCOP pincer receptors, *Dalton Trans.* 46 (2017) 4950–4959.
- [33] G. Jha, N. Anoop, A. Rahaman, M. Sarkar, Fluoride ion sensing in aqueous medium by employing nitrobenzoxadiazole-postgrafted mesoporous silica nanoparticles (MCM-41),

- Phys. Chem. Chem. Phys. 17 (2015) 3525-3533.
- [34] M. J. Langton, C. J. Serpell, P. D. Beer, Anion Recognition in Water: Recent Advances from a Supramolecular and Macromolecular Perspective, *Angew. Chem. Int. Ed.* 55 (2016) 1974-1987.
- [35] R. Kaushik, A. Ghosh, A. Singh, P. Gupta, A. Mittal, D. A. Jose, Selective Detection of Cyanide in Water and Biological Samples by an Off-the-Shelf Compound, *ACS Sens.* 1 (2016) 1265-1271.
- [36] N. Kumari, S. Jha, S. Bhattacharya, Colorimetric Probes Based on Anthraimidazolediones for Selective Sensing of Fluoride and Cyanide Ion via Intramolecular Charge Transfer, *J. Org. Chem.* 76 (2011) 8215-8222.
- [37] Q. Shu, L. Birlenbach, M. Schmittel, A Bis(ferrocenyl)phenanthroline Iridium(III) Complex as a Lab-on-a-Molecule for Cyanide and Fluoride in Aqueous Solution, *Inorg. Chem.* 51 (2012) 13123-13127.
- [38] R. M. F. Batista, E. Oliveira, S. P. G. Costa, C. Lodeiro, M. M. M. Raposo, Cyanide and fluoride colorimetric sensing by novel imidazo-anthraquinones functionalised with indole and carbazole, *Supramol. Chem.* 26 (2014) 71-80.
- [39] H. J. Lee, S. J. Park, H. J. Sin, Y. J. Na, C. Kim, A selective colorimetric chemosensor with an electron-withdrawing group for multi-analytes CN^- and F^- , *New J. Chem.* 39 (2015) 3900-3907.
- [40] A. Mohammadi, Z. Dehghan, M. Rassa, N. Chaibakhsh, Colorimetric probes based on bioactive organic dyes for selective sensing of cyanide and fluoride ions, *Sens. Actuators, B: Chem.* 230 (2016) 388-397.
- [41] A. D. S. Schramm, C. R. Nicoletti, R. I. Stock, R. S. Heying, A. J. Bortoluzzi, V. G. Machado, Anionic optical devices based on 4-(nitrostyryl)phenols for the selective detection of fluoride in acetonitrile and cyanide in water, *Sens. Actuators, B: Chem.* 240 (2017) 1036-1048.
- [42] S. S. Razi, R. Ali, P. Srivastava, A. Misra, Simple Michael acceptor type coumarin derived turn-on fluorescence probes to detect cyanide in pure water, *Tetrahedron Lett.* 55 (2014) 2936-2941.

- [43] S.Y. Xu, X. Sun, H. Ge, R. L. Arrowsmith, J. S. Fossey, S. I. Pascu, Y. B. Jiang, T. D. James, Synthesis and evaluation of a boronate-tagged 1,8-naphthalimide probe for fluoride recognition, *Org. Biomol. Chem.* 13 (2015) 4143-4148.
- [44] L. Zang, D. Wei, S. Wang, S. Jiang, A phenolic Schiff base for highly selective sensing of fluoride and cyanide via different channels, *Tetrahedron.* 68 (2012) 636-641.
- [45] S. Sharma, M. S. Hundal, and G. Hundal, Dual channel chromo/fluorogenic chemosensors for cyanide and fluoride ions—an example of in situ acid catalysis of the Strecker reaction for cyanide ion chemodosimetry, *Org. Biomol. Chem.* 11 (2013) 654-661.
- [46] Y. Sun, Y. Liu, M. Chen, W. Guo, A novel fluorescent and chromogenic probe for cyanide detection in water based on the nucleophilic addition of cyanide to imine group, *Talanta,* 80 (2009) 996-1000.
- [47] S. S. Razi, P. Srivastava, R. Ali, R. C. Gupta, S. K. Dwivedi, A. Misra, A coumarin-derived useful scaffold exhibiting Cu^{2+} induced fluorescence quenching and fluoride sensing (On–Off–On) via copper displacement approach, *Sens. Actuators, B: Chem.* 209 (2015) 162-171.
- [48] Y. J. Na, G. J. Park, H. Y. Jo, S. A. Lee, C. Kim, A colorimetric chemosensor based on a Schiff base for highly selective sensing of cyanide in aqueous solution: the influence of solvents, *New J. Chem.* 38 (2014) 5769-5776.
- [49] J. H. Hu, J. B. Li, J. Qi, Y. Sun, Selective colorimetric and “turn-on” fluorimetric detection of cyanide using an acylhydrazone sensor in aqueous media, *New J. Chem.* 39 (2015) 4041-4046.
- [50] P. Kalpana, S. Suganya, S. Velmathi, Structurally simple azo based chromogenic R1 for the selective sensing of cyanide ion in aqueous medium, *Spectrochim. Acta A Mol. Biomol. Spectrosc.* 171 (2017) 162-167.
- [51] S. N. Sahu, S. K. Padhan, P. K. Sahu, Coumarin functionalized thiocarbonohydrazones as a new class of chromofluorescent receptors for selective detection of fluoride ion, *RSC Adv.* 6 (2016) 90322-90330.
- [52] S. K. Sahu, A. Mishra, R. K. Behera, Synthesis of thiazole, benzothiazole, oxadiazole, thiadiazole, triazole and thiazolidinone incorporated coumarins, *Indian J. Heterocycl. Chem.* 6 (1996) 91–94.

- [53] R. Ahlrichs, et al. TURBOMOLE, (since 1988), version 5.9.1; University of Karlsruhe: Karlsruhe, Germany.
- [54] O. Treutler, R. Ahlrichs, Efficient molecular numerical integration schemes, *J. Chem. Phys.* 102 (1995) 346-354.
- [55] K. Eichkorn, O. Treutler, H. Ohm, M. Haser, R. Ahlrichs, Auxiliary basis sets to approximate Coulomb potentials, *Chem. Phys. Lett.* 242 (1995) 652-660.
- [56] A. D. Becke, Density-functional exchange-energy approximation with correct asymptotic behavior, *Phys. Rev. A.* 38 (1988) 3098-3100.
- [57] C. Lee, W. Yang, R. G. Parr, Development of the Colle-Salvetti correlation-energy formula into a functional of the electron density, *Phys. Rev. B: Condens. Matter Mater. Phys.* 37 (1988) 785-789.
- [58] A. Schafer, C. Huber, R. Ahlrichs, Fully optimized contracted Gaussian basis sets of triple zeta valence quality for atoms Li to Kr, *J. Chem. Phys.* 100 (1994) 5829-5835.
- [59] K. Eichkorn, F. Weigend, O. Treutler, R. Ahlrichs, Auxiliary basis sets for main row atoms and transition metals and their use to approximate Coulomb potentials, *Theor. Chem. Acta.*, 97 (1997) 119-124.
- [60] M. Sierka, A. Hogeckamp, R. Ahlrichs, Fast evaluation of the Coulomb potential for electron densities using multipole accelerated resolution of identity approximation, *J. Chem. Phys.* 118 (2003) 9136-9148.
- [61] S. O. Kang, D. Powell, V. W. Day, K. Bowman-James, Trapped Bifluoride, *Angew. Chem., Int. Ed.* 45 (2006) 1921-1925.
- [62] J. M. Llinares, D. Powell, K. Bowman-James, Ammonium based anion receptors, *Coord. Chem. Rev.* 240 (2003) 57-75.
- [63] S. Gronert, The potential energy surfaces of the identity reactions of the first- and second-row non-metal hydrides with their conjugate bases, *J. Am. Chem. Soc.* 115 (1993) 10258-10266.
- [64] S. Saha, A. Ghosh, P. Mahato, S. Mishra, S. K. Mishra, E. Suresh, S. Das, A. Das, Specific Recognition and Sensing of CN^- in Sodium Cyanide Solution, *Org. Lett.* 12 (2010) 3406-

3409.

- [65] C. E. Housecroft, A. G. Sharpe, *Inorganic Chemistry*, 3rd ed.; Pearson Education, Ltd.: Harlow, (2008) p-537
- [66] D. S. Kim, K. H. Ahn, Fluorescence “Turn-On” Sensing of Carboxylate Anions with Oligothiophene-Based *o*-(Carboxamido)trifluoroacetophenones, *J. Org. Chem.* 73 (2008) 6831–6834.
- [67] R. M. Duke, T. Gunnlaugsson, 3-Urea-1, 8-naphthalimides are good chemosensors: a highly selective dual colorimetric and fluorescent ICT based anion sensor for fluoride, *Tetrahedron Lett.* 52 (2011) 1503–1505.
- [68] J. Xiong, L. Sun, Y. Liao, G. N. Li, J. L. Zuo, X. Z. You, A new optical and electrochemical sensor for fluoride ion based on the functionalized boron–dipyrromethene dye with tetrathiafulvalene moiety, *Tetrahedron Lett.* 52 (2011) 6157–6161.
- [69] J. Y. Kwon, Y. J. Jang, S. K. Kim, K. H. Lee, J. S. Kim, J. Yoon, Unique Hydrogen Bonds between 9-Anthracenyl Hydrogen and Anions, *J. Org. Chem.* 69 (2004) 5155–5157.
- [70] A. K. Mahapatra, P. Karmakar, J. Roy, S. Manna, K. Maiti, P. Sahoo, and D. Mandal, Colorimetric and ratiometric fluorescent chemosensor for fluoride ions based on phenanthroimidazole (PI): spectroscopic, NMR and density functional studies, *RSC Adv.* 5 (2015) 37935–37942.
- [71] V. Thiagarajan, P. Ramamurthy, D. Thirumalai, V. T. Ramakrishnan, A Novel Colorimetric and Fluorescent Chemosensor for Anions Involving PET and ICT Pathways, *Org. Lett.* 7 (2005) 657–660.
- [72] C. Yang, J. Xu, W. Chen, M. Lu, Y. Li, X. Wang, A novel colorimetric and fluorescent sensor for fluoride detection based on a three-arm phenanthroline derivative, *J. Mater. Sci.* 49 (2014) 7040–7048.
- [73] Y. Shiraishi, H. Maehara, T. Sugii, D. Wang, T. Hirai, A BODIPY–indole conjugate as a colorimetric and fluorometric probe for selective fluoride anion detection, *Tetrahedron Lett.* 50 (2009) 4293–4296.
- [74] S. H. Kim, S. Y. Lee, S. Y. Gwon, J. S. Bae, and Y. A. Son, The synthesis and spectral properties of a stimuli-responsive D– π –A charge transfer dye based on indole donor and 2-

cyanomethylene-3-cyano-4,5,5-trimethyl-2,5-dihydrofuran acceptor moieties, *J. Photochem. Photobiol. A.* 217 (2011) 224–227.

- [75] *Guideline for Drinking water Quality*, World Health Organization, Geneva, 1996.
- [76] *Guidelines for Drinking-Water Quality*, 3rd ed., World Health Organization, Geneva, 2004.
- [77] M. Orojloo, S. Amani, Naked-eye detection of cyanide ions in aqueous media based on an azo-azomethine chemosensor, *C. R. Chim.* 20 (2017) 415-423.
- [78] S. S. Razi, R. Ali, P. Srivastava, A. Misra, Simple Michael acceptor type coumarin derived turn-on fluorescence probes to detect cyanide in pure water, *Tetrahedron Lett.* 55 (2014) 2936–2941.
- [79] *Ullmann's Encyclopedia of Industrial Chemistry*, 6th ed., Wiley-VCH, New York, 1999.

Biographies:

Subrata Kumar Padhan obtained his M.Sc. and M.Phil. degree in Chemistry in 2007 and 2010 respectively from Sambalpur University, Odisha, India. He is presently working for his Ph. D. degree at School of Chemistry, Sambalpur University. His research interest mainly involves synthesis of chromogenic and fluoregenic ion sensors.

Mana Bhanjan Podh obtained his M. Phil. degree in Chemistry in 2015 from School of Chemistry, Sambalpur University. He was working on a project on the synthesis of functionalized coumarins.

Prabhat K. Sahu has completed his M. Sc. (Physical Chemistry) and M. Phil. (Theoretical Chemistry) from Sambalpur University, India. He has completed his Ph. D. in Computational Chemistry from National Chung Cheng University, Chia-Yi, Taiwan in 2006. He has received the prestigious Alexander von Humboldt Fellowship in 2007 and also received the National Science Council Taiwan Post-Doctoral Fellowship and German Research Foundation Post-Doctoral Fellowship in the year 2009 and 2010 respectively. Currently, he is heading the Center for Multiscale Modelling at National Institute of Science and Technology, Berhampur, Odisha. His research area includes Bioinformatics, Physical Organic Chemistry, Moletronics and Graph Theory.

Satya Narayan Sahu earned his M.Sc. degree in Chemistry from Utkal University, India, in 2001 and received his M.Tech. degree in Modern Methods of Chemical Analysis in 2003 and Ph.D. degree in Organic Chemistry in 2009 from Indian Institute of Technology, Delhi. After completion of his Ph.D. he joined Sambalpur University, India, as an Assistant Professor in Chemistry, and then moved to Bielefeld University, Germany for post-doctoral work after receiving the BOYSCAST fellowship in 2010 from the Department of Science and Technology, Government of India. His current research interest focuses on the synthesis of chromofluorescent molecular sensors for ionic recognitions.

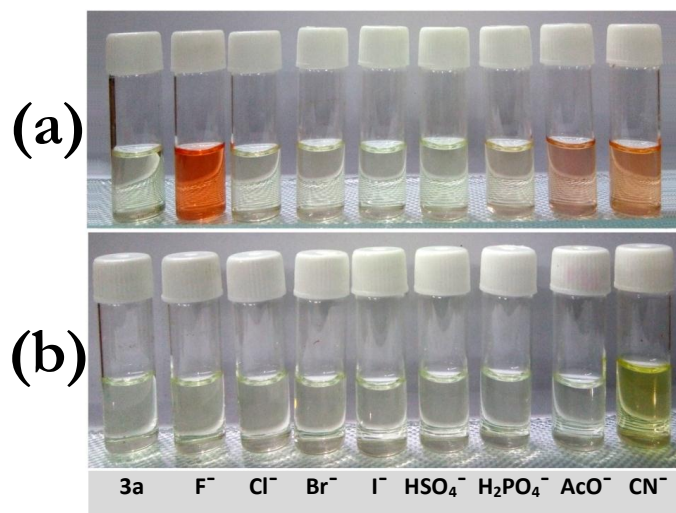


Figure 1: Colorimetric response of probe **3a** in presence of various anions. Colour changes in (a) organic and (b) aqueous solution ($50\mu\text{M}$) with the addition of 10 equivalents of various anions.

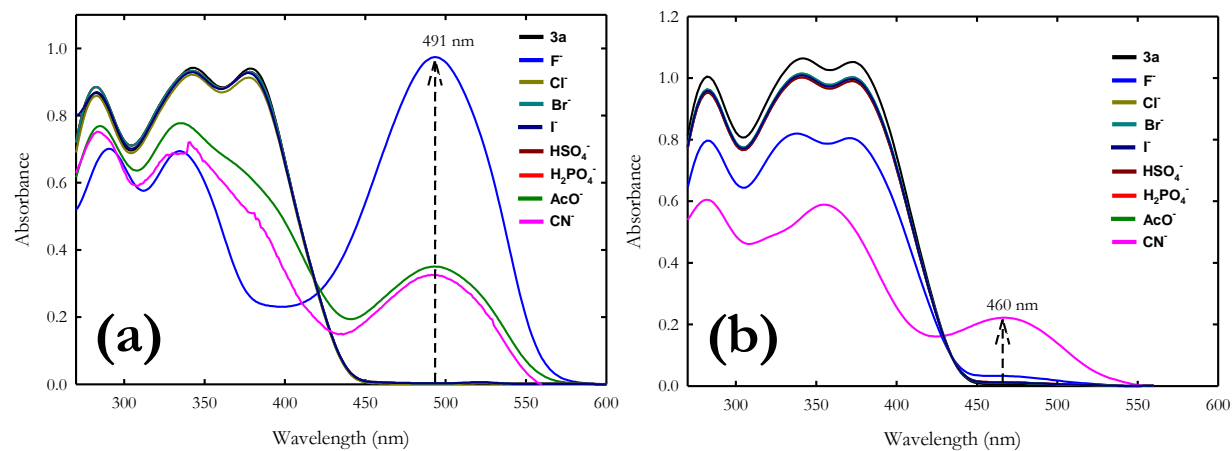


Figure 2: Absorption spectra of probe **3a** upon addition of 10 equiv. of F^- , Cl^- , Br^- , I^- , H_2PO_4^- , HSO_4^- , AcO^- and CN^- ions in (a) organic and (b) aqueous medium ($50\mu\text{M}$).

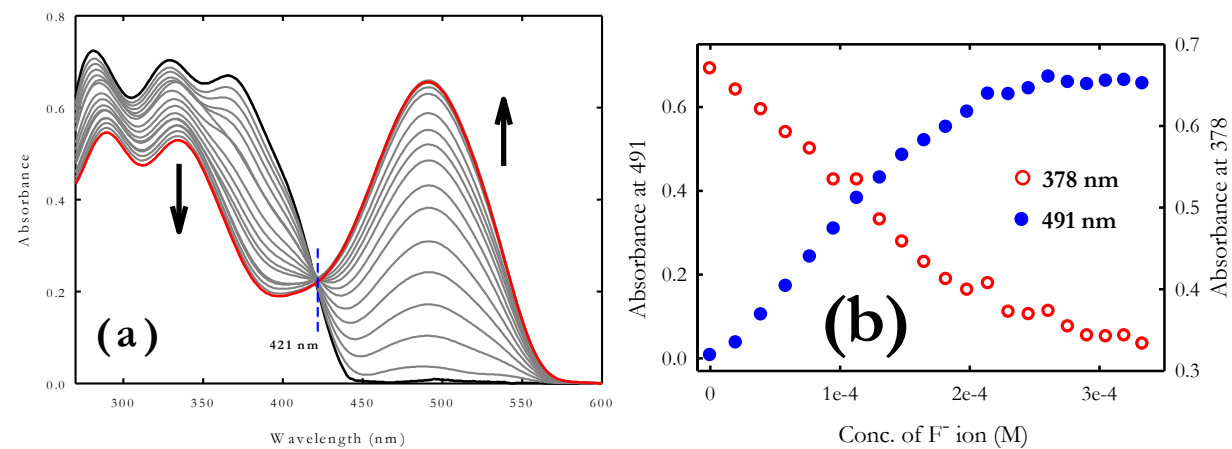


Figure 3: (a) UV-visible titration spectra of probe **3a** ($50\mu\text{M}$) with 0–5 equiv. of TBAF in organic medium, (b) Change in absorbance at 378 and 491 nm with various concentrations of F^- ions.

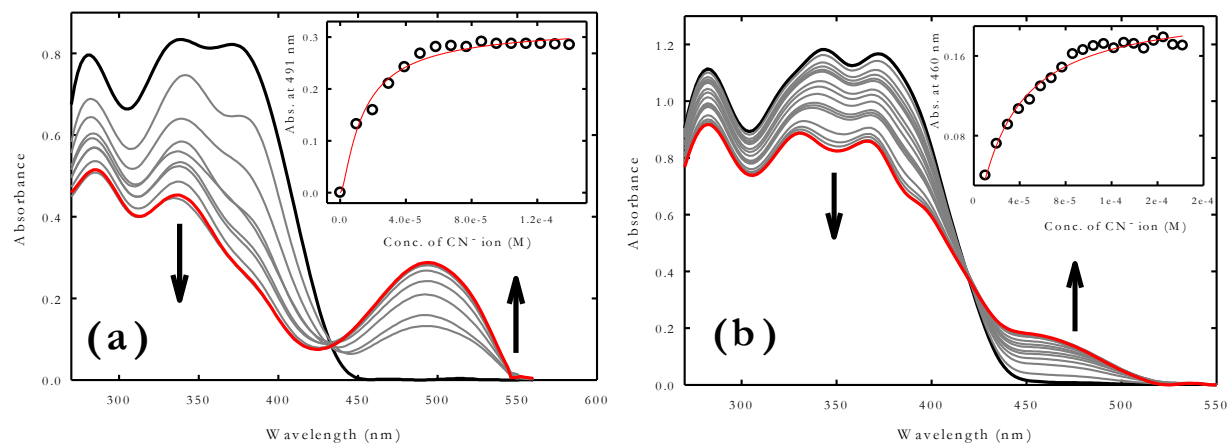


Figure 4: (a) UV-visible titration spectra of probe **3a** (50 μM) with 0–5 equiv. of CN⁻ ion in (a) organic, (b) aqueous medium. Inset shows change in absorbance at 491 nm (a) and 460 nm (b) for **3a** with varying conc. of CN⁻ ion.

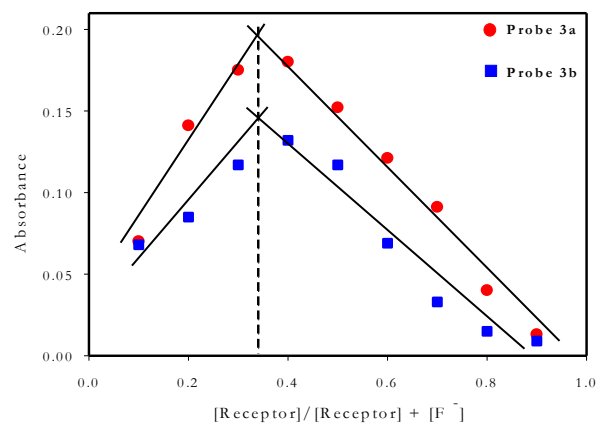


Figure 5: Job's plot for complexation of **3a** (491 nm) and **3b** (494 nm) with F⁻ ions determined by UV-visible experiments in organic medium.

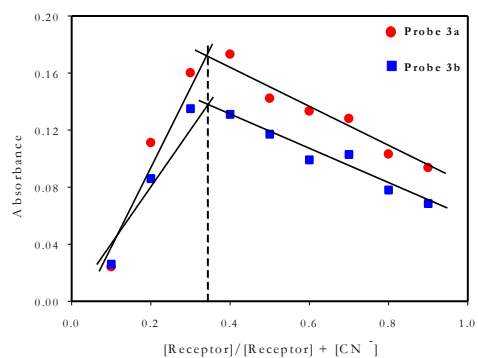


Figure 6: Job's plot for complexation of **3a** (491 nm) and **3b** (494 nm) with CN⁻ ions determined by UV-visible experiments in organic medium.

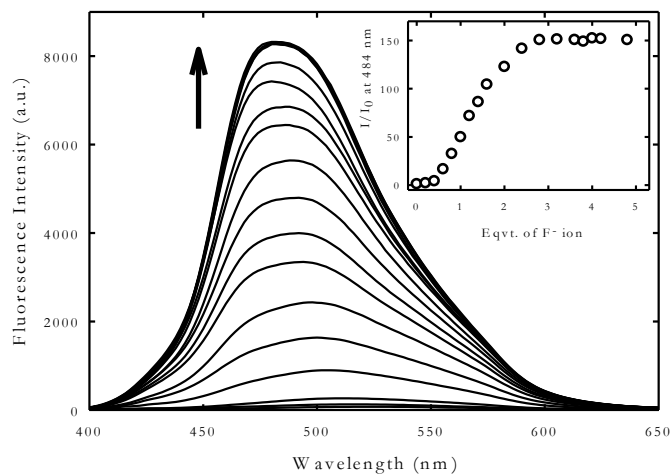


Figure 7: (a) Fluorescence titration spectra of probe **3a** ($50 \mu\text{M}$) with 0–5 equiv. of TBAF in organic medium. Inset shows change in fluorescent intensity (I/I_0) at 484 nm for **3a** with varying equivalents of F^- ion. $\lambda_{\text{ex}} = 375 \text{ nm}$, $\lambda_{\text{em}} = 484 \text{ nm}$.

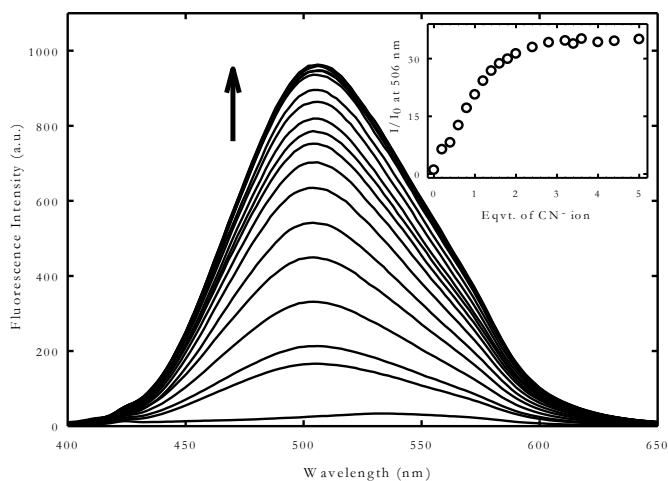


Figure 8: Fluorescence titration spectra of probe **3a** ($50 \mu\text{M}$) with 0–5 equiv. of CN^- in aqueous medium. Inset shows change in fluorescent intensity (I/I_0) at 506 nm for **3a** with varying equivalents of CN^- ion. $\lambda_{\text{ex}} = 375 \text{ nm}$, $\lambda_{\text{em}} = 506 \text{ nm}$.

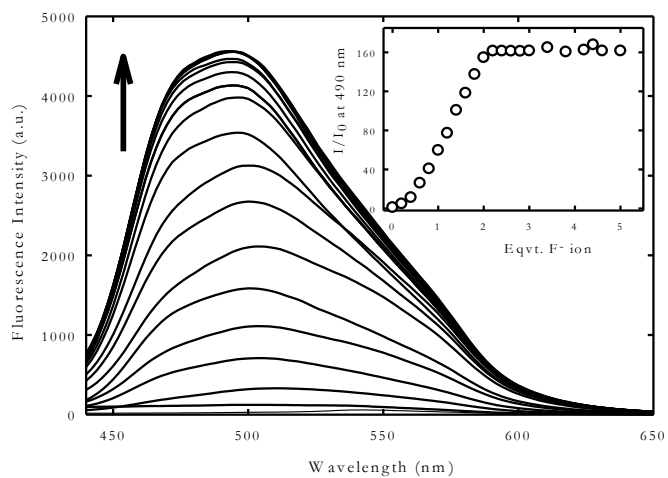


Figure 9: Fluorescence titration spectra of probe **3b** ($50 \mu\text{M}$) with 0–5 equiv. of TBAF in organic medium. Inset shows change in fluorescent intensity (I/I_0) at 490 nm for **3b** with varying equivalents of F^- ion. $\lambda_{\text{ex}} = 375 \text{ nm}$, $\lambda_{\text{em}} = 490 \text{ nm}$.

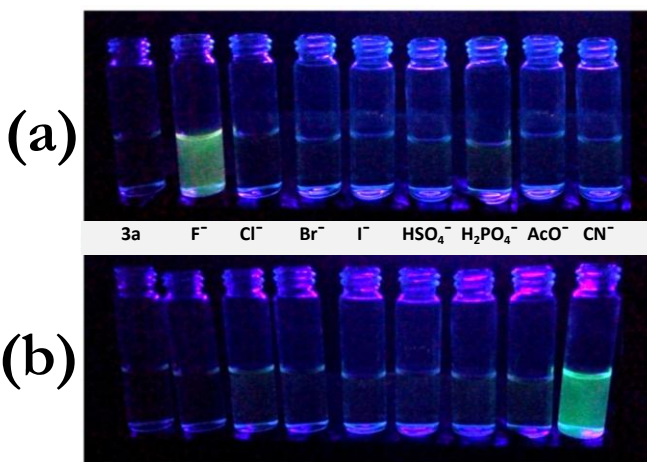


Figure 10: Fluorescent “turn on” behaviour of **3a** ($50 \mu\text{M}$) for (a) fluoride ion in organic medium (b) cyanide ion in aqueous medium over other anions (10 equivalents) under UV light (365 nm).

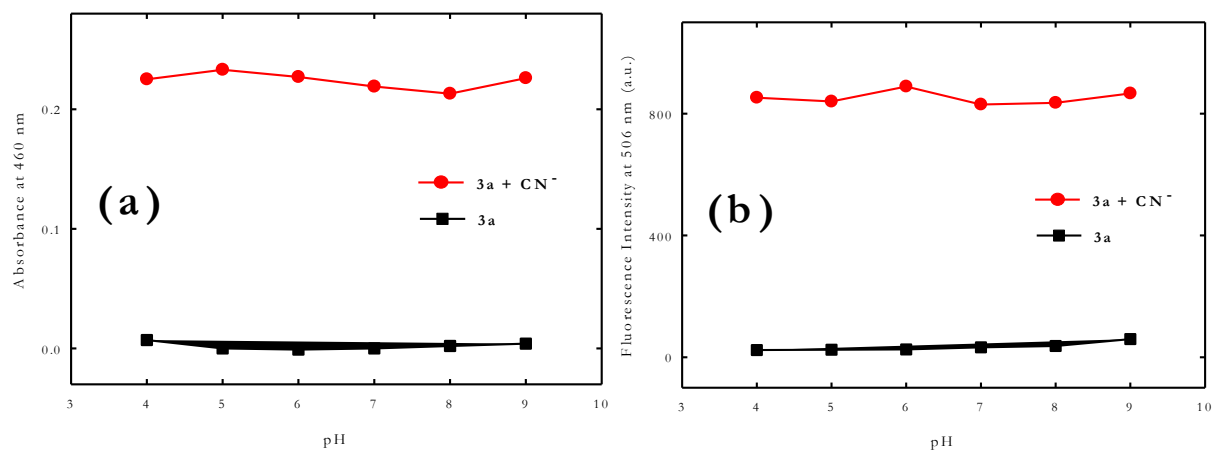


Figure 12: Effect of pH on the absorbance (a) and emission (b) spectra of probe **3a** (50 μM) containing 10 equiv. of CN^- ions.

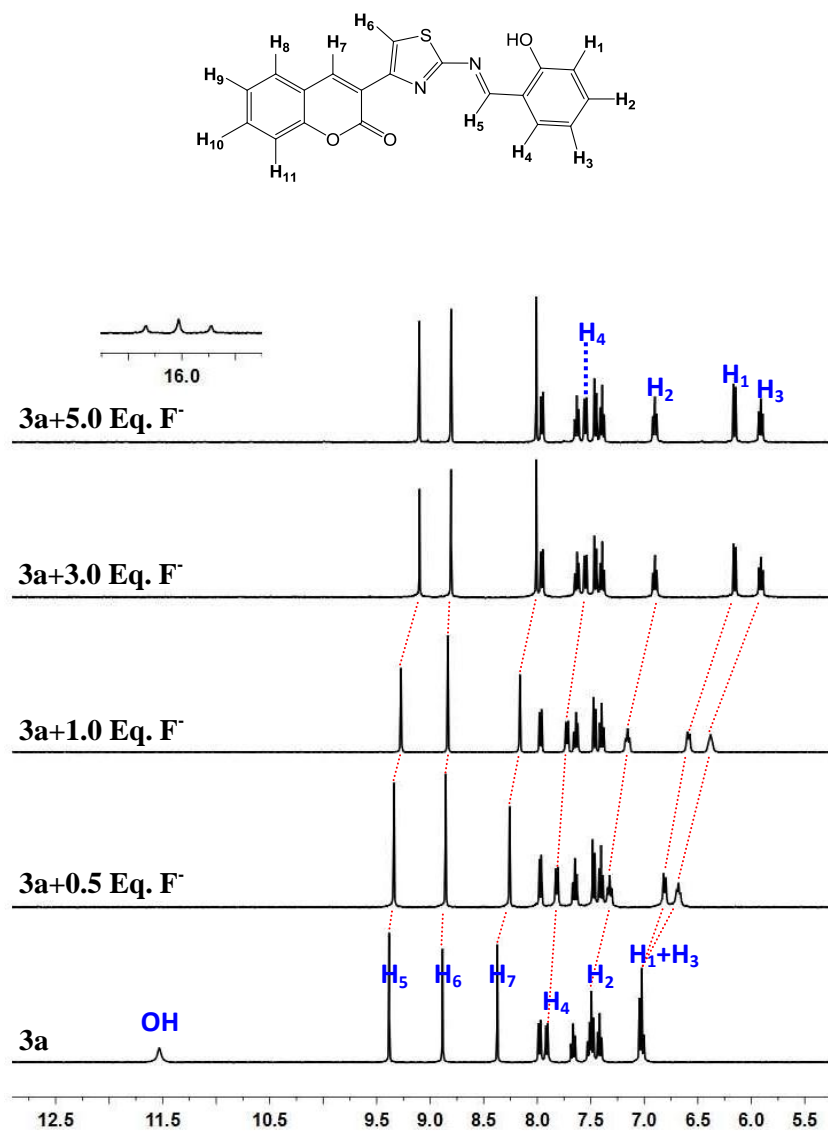


Figure 13: ^1H NMR titration spectra of probe **3a** (5 mM) upon addition of various equivalents of F^- ion in DMSO-d_6 .

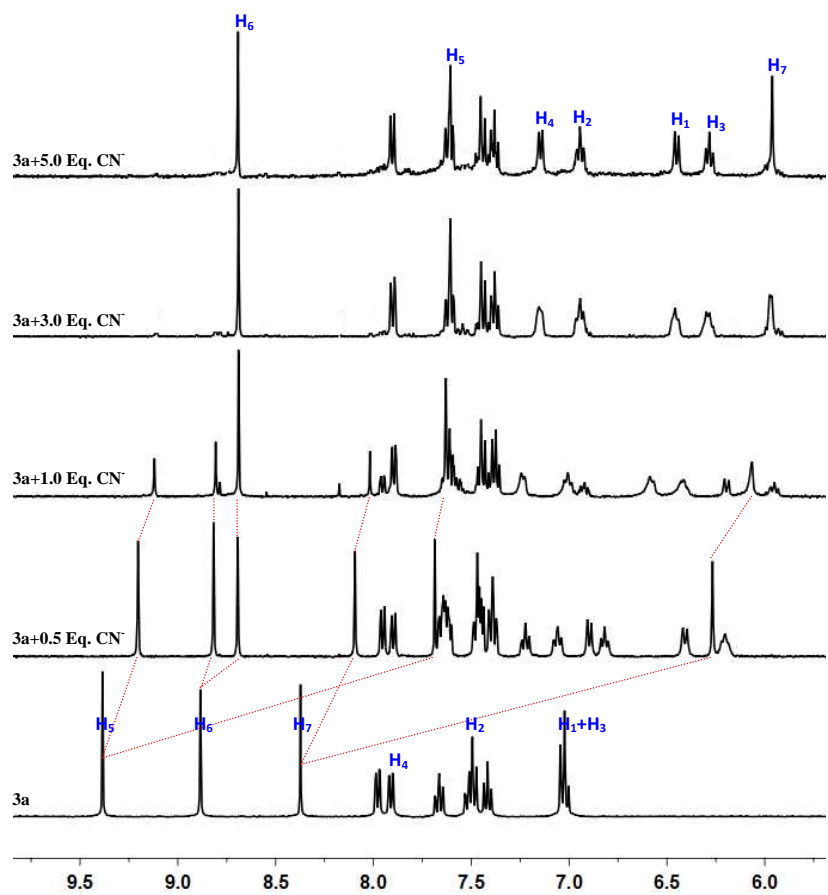


Figure 14: ^1H NMR titration spectra of the probe **3a** (5 mM) upon addition of various equivalents of CN^- ion in DMSO-d_6 .

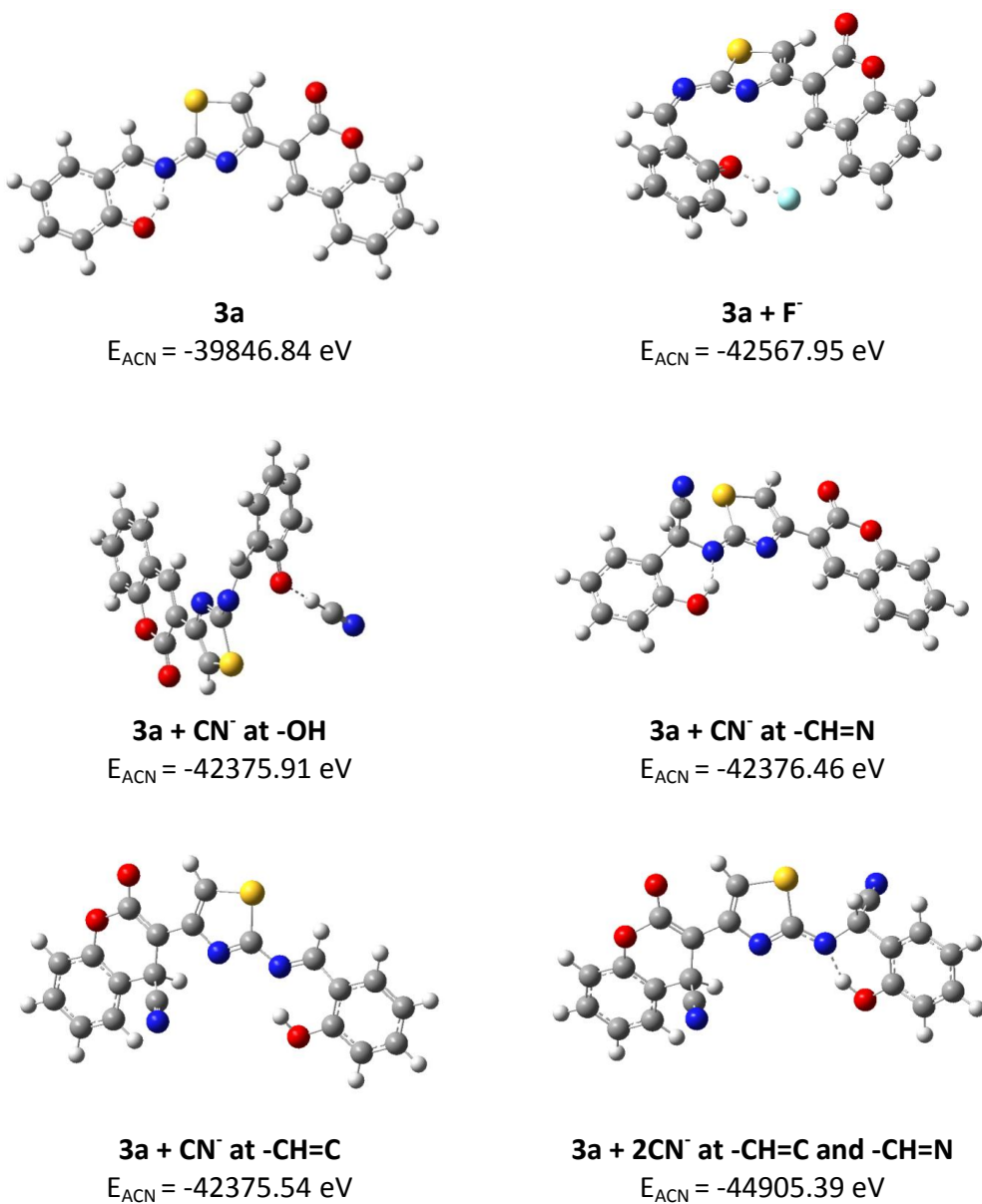


Figure 15: Optimized structures of probe **3a** and its complexes with fluoride and cyanide ions at the indicated positions (colour key: white = hydrogen; grey = carbon; blue = nitrogen; red = oxygen; yellow = sulfur; cyan = fluorine). E_{ACN} indicates the calculated total energy in acetonitrile solvent system.

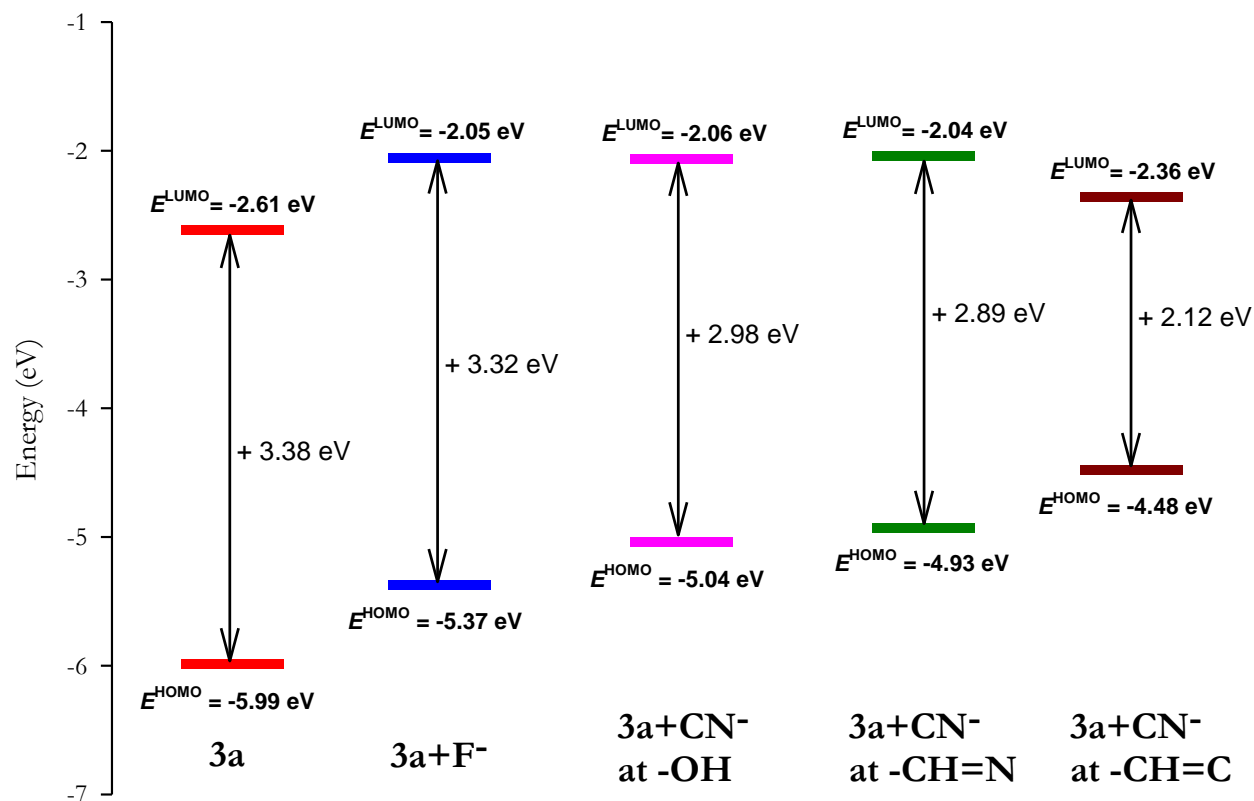


Figure 16: Energy diagrams of HOMO and LUMO orbital of **3a** and its complexes with fluoride and cyanide ions calculated on the DFT level using a B3LYP/TZVP(RI) basis set.

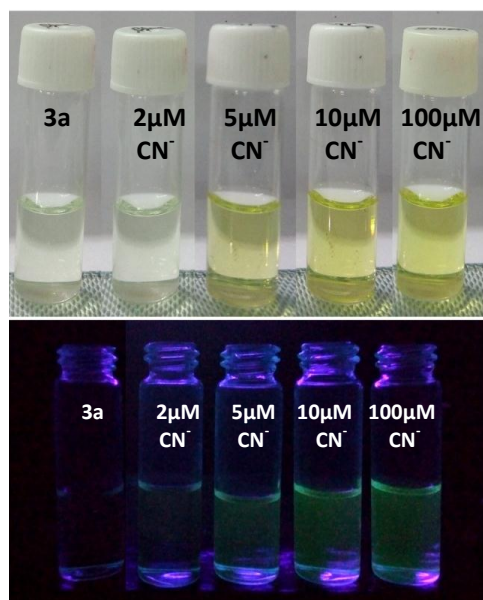
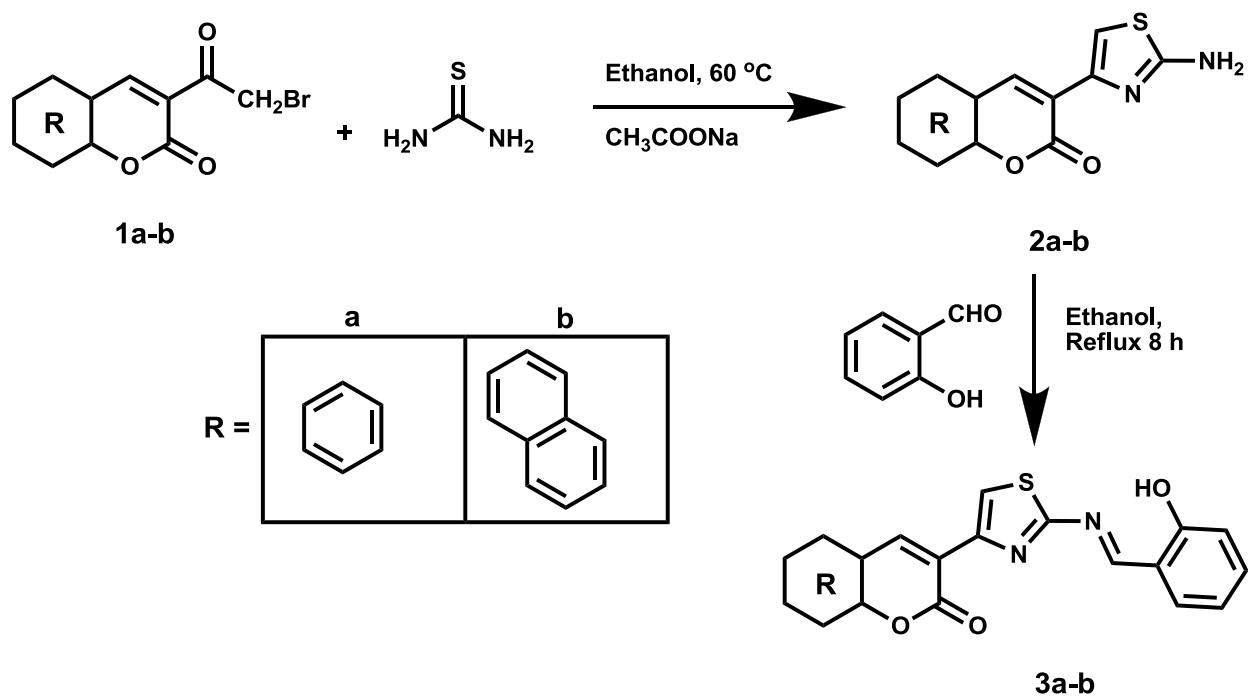
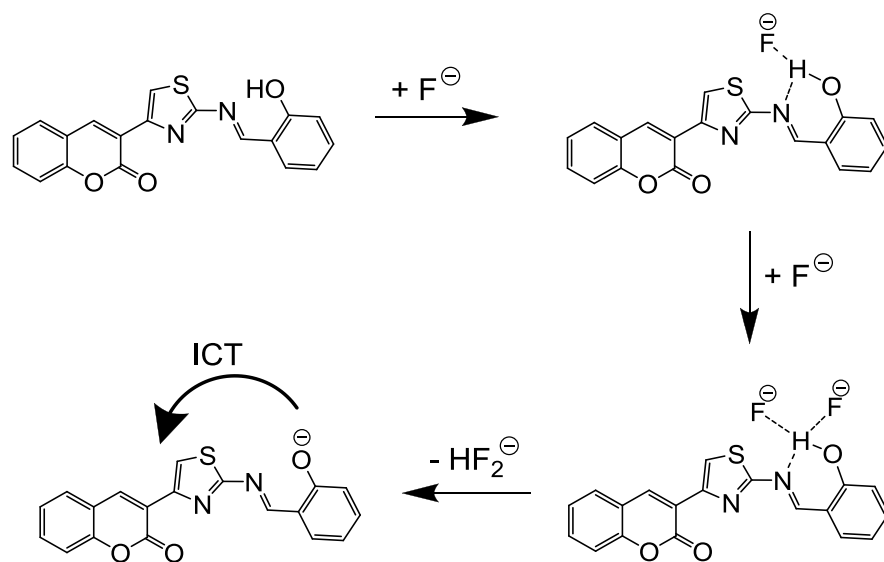


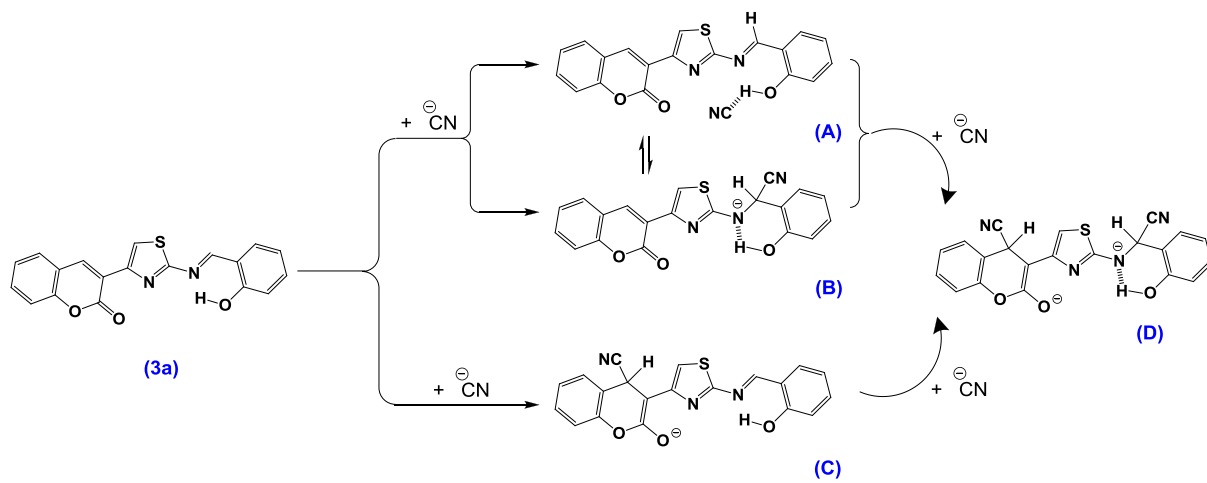
Figure 17: Visual colour (top) and fluorescence change (bottom under UV light 365 nm) of **3a** (50 μM) with the addition of various concentration of CN^- ion in tap water.



Scheme 1: Synthesis of probes **3a** and **3b**.



Scheme 2: A proposed binding mode and deprotonation of probe **3a** in the presence of fluoride ions.



Scheme 3: A proposed binding mode of probe **3a** in the presence of cyanide ions.